Rivista Italiana di Paleontologia e Stratigrafia
(*Research in Paleontology and Stratigraphy*)
vol. 132(2): 269-293. **July 2026**
DOI: https://doi.org/10.54103/2039-4942/30524

REFINED STRATIGRAPHICAL AND BIOCHRONOLOGICAL FRAMEWORK OF PALEOGENE SUCCESSIONS IN THE NORTHWEST ARABIAN PLATE

MOHAMMED H. ALJAHDALI[1], IBRAHIM M. GHANDOUR[1&2], MAHMOUD FARIS[2], RASHAD A. BANTAN[1], MAZEN M. ALSADDAH[1], KHALID M. ALRIZQI[1], BRIDGET WADE[3] & RAMADAN M. EL-KAHAWY[4*]

[1]Department of Marine Geology, Faculty of Marine Sciences, King Abdulaziz University, Jeddah, 21589, Saudi Arabia.
E-mail: maljahdli@kau.edu.sa; ighandour@kau.edu.sa; rbantan@kau.edu.sa; kalrizqI0002@stu.kau.edu.sa; malsaddah0003@stu.kau.edu.sa
[2]Geology Department, Faculty of Science, Tanta University, Tanta, 31527, Egypt.
E-mail: mhmfaris@yahoo.com; ibrahim.ghandour@science.tanta.edu.eg
[3]Department of Earth Sciences, University College London, Gower Street, London, WCIE 6BT, UK. E-mail: b.wade@ucl.ac.uk
[4]Geology Department, Faculty of Science, Cairo University, Cairo 13615, Egypt. E-mail: relkahawy@cu.edu.eg
*Corresponding author.

Associate Editor: Silvia Gardin.

To cite this article: Aljahdali M.H., Ghandour I.M., Faris M., Bantan R.A., Mazen M. Alsaddah M.M., Alrizqi K.M., Wade B. & El-Kahawy R.M. (2026) - Refined stratigraphical and biochronological framework of Paleogene successions in the northwest Arabian Plate. *Rivista Italiana di Paleontologia e Stratigrafia*, vol. 132(2): 269-293.

Key words: Rashrashiyah Formation; Sirhan-Turayf Basin; Eocene-Oligocene; Arabian Plate; Calcareous nannofossils; Differential subsidence.

Abstract. This study updates the lithostratigraphic and chronostratigraphic framework of the marine carbonate-dominated Paleogene strata of northwestern Saudi Arabia within the Sirhan–Turayf Basin by integrating detailed field observations and high-resolution calcareous nannofossil biostratigraphy. Previous studies assigned these strata to the Middle–Upper Eocene Rashrashiyah Formation but lacked precise chronostratigraphic constraints. New biostratigraphic and lithostratigraphic data from three measured sections (Rash1–Rash3) reveal that these strata comprise two distinct formations: the Middle–Upper Eocene Rashrashiyah Formation and the newly defined Lower Oligocene Qurayyat Formation, separated by a prominent erosional disconformity at the Eocene–Oligocene boundary (EOB). The revised framework highlights the role of local tectonics, including block faulting and differential subsidence, in preserving the Oligocene strata. Calcareous nannofossil assemblages suggest that the Rashrashiyah Formation corresponds to Zones NP17–NP20, while the Qurayyat Formation is assigned to Zone NP21, collectively spanning the Bartonian–Rupelian interval. The documentation of marine Oligocene strata in NW Saudi Arabia for the first time, with erosional disconformity at the base, challenges previous interpretations of continuous sedimentation across the Eocene-Oligocene transition. The findings suggest that depositional architecture and stratal distribution in the study area are significantly controlled by regional tectonics and global sea-level fluctuations. The proposed lithostratigraphic scheme and chronostratigraphic constraints improve regional correlations across the Arabian Plate.

INTRODUCTION

The Arabian Plate hosts extensive Paleogene carbonate deposits of considerable economic and scientific significance. These deposits constitute major hydrocarbon source and reservoir rocks in the northeastern sector of the plate (Beydoun 1993; Alsharhan & Nairn 1997; Kamali et al. 2006; Bordenave & Hegre 2010; Lawa & Ghafur 2015; Sadooni & Alsharhan 2019), and contain the largest

Received: December 19, 2025; accepted: March 19, 2026

phosphorite accumulations in Saudi Arabia, notably in the Hazm Al-Jalamid and Umm Wu'al areas of the Sirhan–Turayf region (Al-Hobaib et al. 2013; Galmed et al. 2020; Zhang et al. 2021; Ahmed et al. 2022). Beyond their economic value, Paleogene deposits are of global and regional scientific interest, as they record critical paleoenvironmental and climatic changes associated with the progressive closure of the Neo-Tethys Ocean during the Late Eocene–Oligocene (Harzhauser et al. 2002; Lawver & Gahagan 2003; Al-Hobaib et al. 2013; Galmed et al. 2020; Messaoud et al. 2020; Zhang et al. 2021; Ahmed et al. 2022). Furthermore, they contain diverse marine vertebrate assemblages (Zalmout 2023).

The stratigraphy of the Paleogene succession in the Arabian Plate is complex and strongly influenced by eustatic sea-level changes and regional tectonics. The Ha'il Arch divides the Arabian Plate into two basins: the Arabian Basin (Arabian Gulf facies) to the east and the Sirhan-Turayf Basin (Mediterranean facies) to the west. While comprehensive lithostratigraphic schemes and chronostratigraphic interpretations are available for the main Arabian Basin (Beydoun 1988; Alsharhan & Nairn 1997; Christian 1997; Sharland et al. 2001), equivalent data for the Sirhan-Turayf Basin remain scarce. In northwestern Saudi Arabia, little work has been done, and the exact nature of the Paleogene stratigraphy is poorly understood. The Paleogene stratigraphy of Sirhan-Turayf Basin has been previously established relying primarily on field observations and lithology (Meissner et al. 1989), neglecting microfossil content and lateral facies variations.

Geological mapping by the Saudi Geological Survey (SGS) indicates that the oldest exposed deposits in Qa'a Al-Rashrashiyah, east of Al-Qurayyat, belong to the Middle-Upper Eocene Rashrashiyah Formation that is unconformably overlain by the Miocene Sirhan Formation (Meissner et al. 1989). The deposits of the Rashrashiyah Formation are exceptionally rich in well-preserved Upper Eocene planktonic foraminifera and calcareous nannofossils (Aljahdali et al. 2020; Wade et al. 2021).

New stratigraphic findings of equivalent Paleogene strata in Jordan (Farouk et al. 2013; Farouk et al. 2015)3D and Iraq (Al-Banna et al. 2010; Al-Rubai & Al-Mutwali 2020) raise questions regarding the stratigraphy and age of the exposed Paleogene strata in NW Saudi Arabia. Misinterpretations and the absence of reliable biostratigraphic markers in earlier work of Meissner et al. (1989) necessitate a revision and update of these stratigraphic subdivisions. Preliminary findings indicate that previous stratigraphic assignments are inaccurate, underscoring the need for a comprehensive reassessment of the ages and contact relationships of Paleogene units within the Sirhan–Turayf Basin.

This study aims to revise and update the lithostratigraphic framework and the age of the Paleogene strata in the NW Saudi Arabia using calcareous nannofossil records. The results will be correlated with the corresponding strata across the Arabian Plate to establish a more robust regional stratigraphic framework.

Geologic setting

The Arabian Plate is bordered to the northwest by the Dead Sea transform, to the northeast by the Taurus-Zagros crush zone, to the southeast by the Indian Ocean passive/transform margin, and to the southwest by the Red Sea rift margin (Berberian & King 1981; Beydoun 1991; Aldaajani et al. 2021). The rock successions of the Arabian Plate show five complex phases of tectonic evolution, starting with Precambrian accretion and culminating in an active margin setting from the Late Mesozoic to present (Sharland et al. 2001).

During the Paleogene, the Arabian Plate was located along the southern margin of the Neo-Tethys Ocean. This ocean separated the Arabian Plate from the Eurasian Plate to the north (Dercourt 1993). The Arabian Plate was a part of a broad shallow-marine carbonate platform with continuous transgression until the early Middle Eocene (Martín-Martín et al. 2021), followed by significant uplift and regression during the Late Eocene, resulting in a major unconformity between Eocene and Oligocene strata (Whittle et al. 1995), This hiatus reflects the Afro-Arabian–Eurasian collision, closure of the Neo-Tethys, and a global sea-level fall of approximately 70 m (Alsharhan & Nairn 1995; Sharland et al. 2001; Allen et al. 2004; Guiraud et al. 2005; Haq & Al-Qahtani 2005; Al-Husseini 2008; Allen & Armstrong 2008). The Eocene and Oligocene deposits correspond to the Arabian Plate Megasequences AP10 and AP11 (Sharland et al. 2001), separated by a regional unconformity at ~34 Ma.

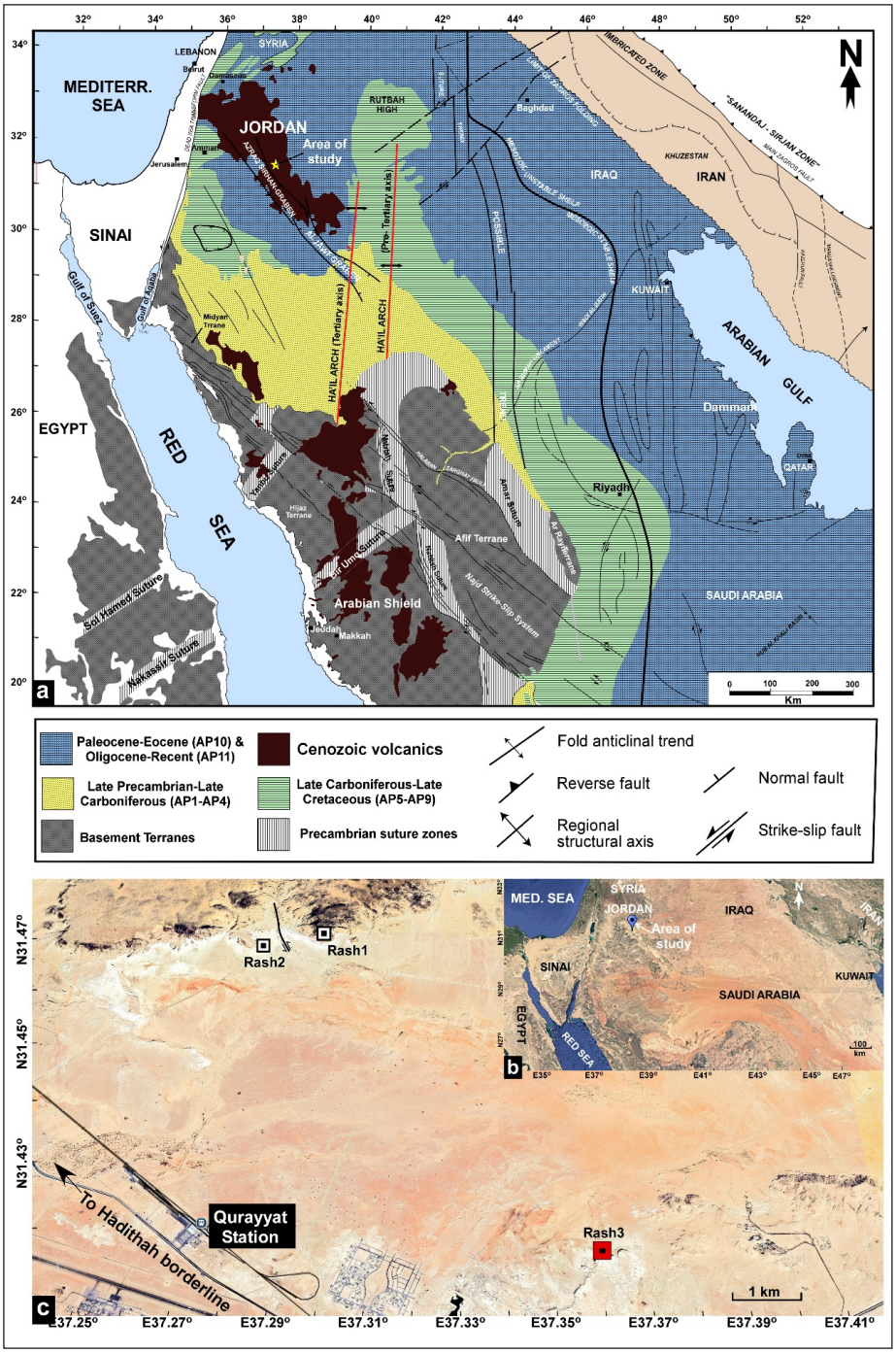

Fig. 1 - a) Schematic geological map of the Arabian Plate showing the main tectonic elements of the Arabian Plate (after Sharland et al., 2001). b and c) Google maps show the locations of the area of study and the investigated sections (Rash1-Rash3), respectively. Note: The red polygon in Figure 1c represents the proposed type section (Rash3) for the Qurayyat Formation.

Two main tectonic domains (Powers et al. 1966) separated by the north-west trending, doubly plunging Ha'il Arch fold complex (Fig. 1a) were recognized in northern Saudi Arabia. The two domains are the eastern or the Arabian Basin (Arabian Gulf facies affinity) and the complex Sirhan-Turayf Basin (Mediterranean Sea facies affinity) that extends into Iraq and Jordan (Powers et al. 1966; El-Khayal 1974). The sedimentary facies and depositional setting varied widely in the two domains. In the Arabian Basin, fine-grained siliciclastics dominate the fore-deep basin in the northeast plate margin in the Zagros and northern United Arab Emirates, whereas shallow marine carbonates filled the basin margin (Sadooni & Alsharhan 2019; Nikfard 2023). The Sirhan-Turayf Basin lies on the western flank of the Hail Arch and forms a homocline dipping gently westward towards the Wadi As-Sirhan graben complex (Meissner et al. 1989). Paleogene deposits in the Sirhan-Turayf basin are exclusively deep to shallow marine carbonates (Powers et al. 1966).

The study area is located in the NW sector of the Arabian Plate (Fig. 1b). It is a part of the Turayf and An Nabk quadrangles in the north-central

part of the Sirhan-Turayf Basin, near the Al-Hadithah borderline with Jordan (Fig. 1b and c). It is situated approximately 16 kilometers from Qa'Al Rashrashiyah, north of An-Nabk, west of Turayf, between latitudes N 31.41° and N 31.47° and longitudes E 37.29° and E 37.39°. The stratigraphic section of the Sirhan-Turayf Basin comprises phosphatic carbonates of the Turayf Group (Late Cretaceous-Middle Eocene) that is subdivided stratigraphically into the Jalamid, Mira, and Umm Wu'al formations (Meissner et al. 1987). The sediments of the Turayf Group are overlain by the Middle-Upper Eocene Rashrashiyah Formation (Meissner et al. 1989). The stratigraphic relationship between the Turayf Group and the overlying Rashrashiyah Formation remains uncertain. The Rashrashiyah Formation displays a lithological similarity with the Jirani Member (upper Umm Wu'al Formation), suggesting a possible lateral facies transition; however, lacking more definitive data and a clear field relationship, the Rashrashiyah is placed stratigraphically above the Jirani Member (Meissner et al. 1989).

The Rashrashiyah Formation consists of white to grey and yellow, thick-and thin-bedded marls, clayey limestones, and chalky limestone deposited in an interior basin. It is unconformably overlain by the siliciclastic-dominated Miocene Sirhan Formation (Meissner et al. 1989). The age of the Rashrashiyah Formation remains poorly constrained. Meissner et al. (1989) assigned the Rashrashiyah Formation to the Middle and Late Eocene and reported no definitive Oligocene strata in the region. Recently, Aljahdali et al. (2020) and Wade et al. (2021) assigned the uppermost part of the Rashrashiyah Formation to the Late Eocene based on calcareous nannofossils and planktonic foraminifera, respectively. Additionally, Abu-Zied et al. (2025), based on planktonic foraminiferal biostratigraphy of four stratigraphic sections in the Rashrashiyah area, were assigned a Middle Eocene-Early Oligocene age documenting continuous sedimentation across the Eocene/Oligocene boundary (EOB).

In contrast to the substantial body of calcareous nannofossil research conducted in the Tethyan realm, particularly in Iran (Senemari & Jalili 2021; Senemari & Mahanipour 2023) and Tunisia (Messaoud et al. 2020; Messaoud et al. 2023), studies focusing on Eocene–Oligocene nannofossil biostratigraphy within the Arabian Plate remain comparatively limited (Farouk et al. 2015; Aljahdali et al. 2020). This scarcity highlights the importance of the present study in refining regional biostratigraphic frameworks and improving correlations across the southern Tethyan margin during a critical interval of global paleoceanographic and climatic changes.

Materials and methods

The lithostratigraphic framework of the Paleogene deposits in the Rashrashiyah area was revised through an integrated traditional fieldwork and calcareous nannofossil biostratigraphy. The study area comprises two sectors, northern and southern (Fig. 1c). The work includes three stratigraphic sections: Rash1 and Rash2 from the northern sector, and Rash3 from the southern sector (Fig. 1c). All sections were systematically measured, described, and sampled. Rash1 and Rash2 were collected from the footwall and hanging wall of a fault trending N45°W, respectively. Sampling intervals ranged from 0.4 to 1 m, depending on lithological changes, with particular attention paid to bed contacts, lithological variations, and discontinuity surfaces.

Smear slides for calcareous nannofossil analysis were prepared following standard procedures (Perch-Nielsen 1985, Bown & Young 1998, Aljahdali et al. 2019). Freshly cut sediment fragments were placed on coverslips, smeared with a rounded toothpick after adding a drop of distilled water, and dried on a low-temperature hotplate. Coverslips were then mounted on glass slides using Norland Optical Adhesive No. 61 and cured under UV light for five minutes (Aljahdali et al. 2019). Microscopic analysis was conducted using a BEL polarizing microscope with a 100× objective lens (1000× magnification). Digital images of nannofossil specimens were captured using a Nikon camera mounted on a Nikon microscope at the Central Laboratory, Geology Department, Faculty of Science, Cairo University, Egypt.

Taxonomic identification followed Perch-Nielsen (1985), Aubry (1984, 1990, 1999), and the Nannotax3 online database (https://www.mikrotax.org/Nannotax3/). Biostratigraphic zonation schemes of Martini (1971), Okada and Bukry (1980), and Agnini et al. (2014) are adopted here. Quantitative analysis was achieved by counting at least 300

specimens per sample. Calcareous nannofossil events assigned the studied sections to Zones NP17–NP21, corresponding to the Bartonian–Rupelian interval. The identified assemblages, generally well-preserved and abundant, include numerous stratigraphic marker species, facilitating precise zonation. Bioevents were defined by the lowest and highest occurrences (LO and HO, respectively) of key index species. The most common nannofossil species are shown in Figures 2-5. Furthermore, the list of identified calcareous nannofossil taxa of the present study is provided in Appendix 1.

Calcareous nannofossil preservation was evaluated qualitatively during microscopic examination following standard criteria based on dissolution, overgrowth, fragmentation, and etching intensity. Specimens were classified into three preservation categories: good (G), where coccolith structures are clearly preserved with minimal dissolution or overgrowth; moderate (M), where partial dissolution or secondary calcite overgrowth affects structural details, but taxa remain identifiable; and poor (P), where strong dissolution, breakage, or recrystallization significantly obscures diagnostic features.

Relative abundance data were calculated from quantitative counts (300 specimens) of identified taxa and expressed as percentages of the total assemblage per sample. Data processing and graphical representations (see Appendices 2-4) were produced using OriginPro (OriginLab Corporation) and R statistical software (R Core Team, 2025), respectively.

Results

Lithostratigraphy

The present study revises and re-evaluates the stratigraphic framework of the fully marine, carbonate-dominated Paleogene strata that are exposed in the northern Qa'a Al-Rashrashiyah, east of Al-Qurayyat, northern Saudi Arabia. The strata were formerly defined as the Rashrashiyah Formation of a Middle-Late Eocene age (Meissner et al. 1989) and the knowledge of its lithologic composition and stratigraphic extent persisted until recently (Aljahdali et al. 2020, Wade et al. 2021, Allam et al. 2025, Korin et al. 2025). Based on field observations and calcareous nannofossil data, Paleogene deposits in this region are subdivided herein into two distinct formations of different ages and lithology: the Middle–Upper Eocene Rashrashiyah Formation, unconformably overlain by the Lower Oligocene Qurayyat Formation.

In the northern sector, two measured sections (Rash1 and Rash2), located approximately 1.2 km apart (Fig. 1c), are separated by a normal fault trending N45°W. The Rash2 section lies on the hanging wall, whereas the Rash1 section lies in the footwall. The typical Rashrashiyah Formation is best exposed at Rash1 (Fig. 6a-d), where it attains a thickness of approximately 52 m and forms a prominent cliff of light grey to white, massive, thick-bedded marl, chalk, and chalky limestone (Fig. 6a). The basal contact is unexposed, while the upper contact is marked by a subaerial unconformity separating it from the overlying siliciclastic-dominated Sirhan Formation (Fig. 6a, d), tentatively assigned a Miocene age. At Rash2 and Rash3, the upper member of the Rashrashiyah Formation is truncated by an erosional disconformity characterized by *Glossifungites* ichnofacies, which defines the contact with the overlying Qurayyat Formation.

Although macrofossils are absent, trace fossils occur at several stratigraphic levels. The Rashrashiyah Formation is informally subdivided into three members based on lithological characteristics. The lower and middle members are defined at Rash1, whereas the upper member occupies the upper part of Rash1 and the basal portions of Rash2 and Rash3 (Fig. 6a, e). The lower member consists mainly of soft marl to chalk beds, 3 and 6 m thick; each ends with a distinctive grey-coloured horizons (30-50 cm thick) densely burrowed by branches of *Thalassinoides* trace fossils (Fig. 6b). The second grey horizon (Fig. 6a) marks the boundary with the middle member, which consists of thick-bedded chalky limestone containing grey to greenish-grey barite nodules of variable size and shape (Fig. 6c). The upper member is composed of white, thick-bedded limestone, locally argillaceous and sparsely burrowed by vertical burrows. The upper member of the Rashrashiyah Formation in Rash1 is time equivalent to that at the base of sections Rash2 and Rash3.

The newly introduced Qurayyat Formation differs substantially from the underlying Rashrashiyah Formation and deserves to be treated differently from the rest of the succession. The present study raised the carbonate rocks overlying the

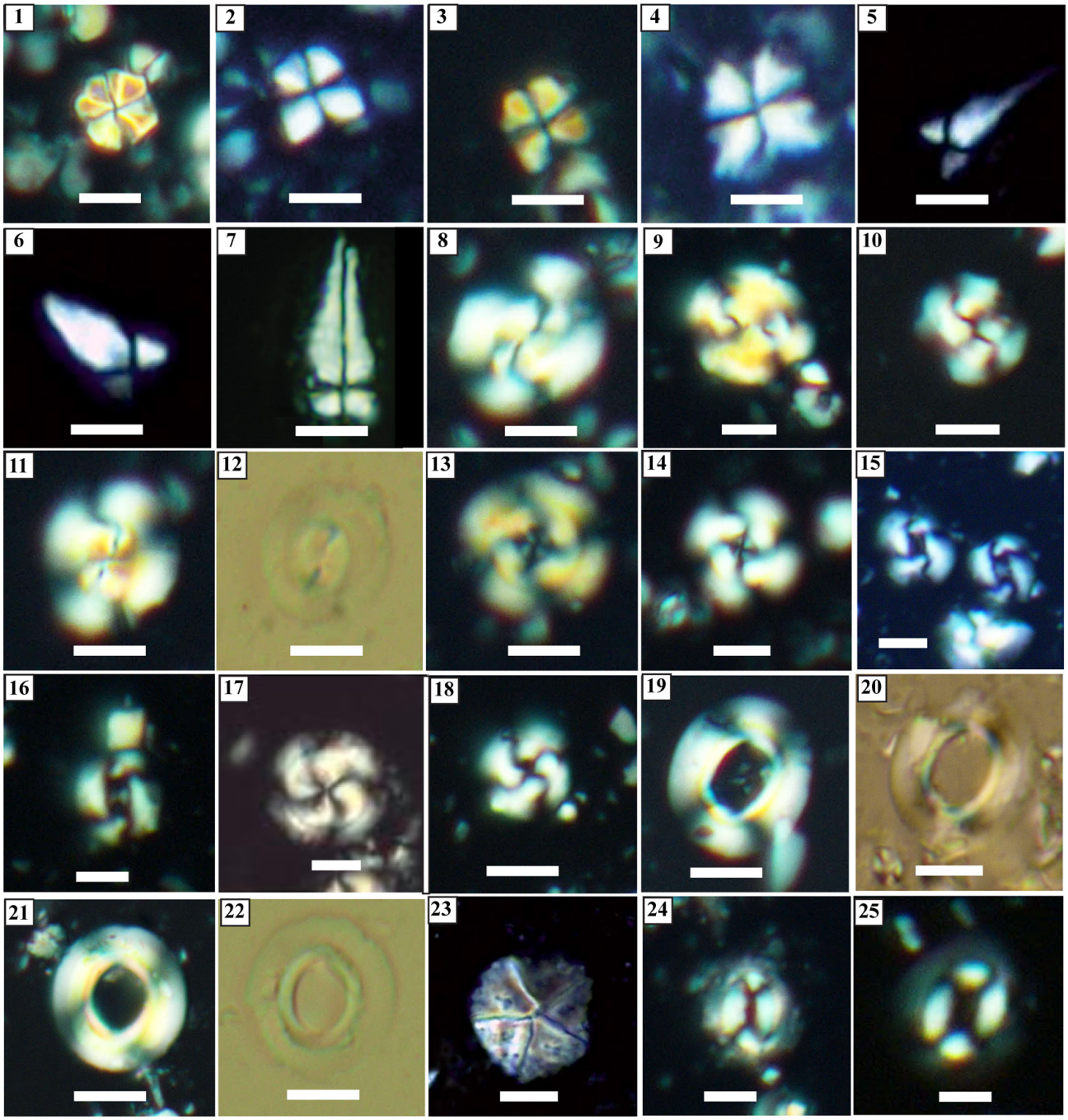

Fig. 2 - Photomicrographs for calcareous nannofossil taxa retrieved from the investigated sections of the Rashrasheyia area, the bar scale is equivalent to 5µm, 1. *Sphenolithus puniceus*, Sample Rash3-1, Zone NP19/20, 2-4. *Sphenolithus moriformis*, Sample Rash1-3, NP17 Zone, 5-6. *Furcatolithus obtusus*, Sample Rash1-13, Zone NP17, 7. *Sphenolithus pseudoradians*, Sample Rash1-26, Zone NP17, 8-12. *Reticulofenestra bisecta*, Sample Rash2-4, Zone NP19/20, 13-14. *Reticulofenestra reticulata*, Sample Rash2-6, Zone NP19/20, 15-16. *Reticulofenestra lockeri*, Sample Rash1-11, Zone NP17, 17-18. *Reticulofenestra erbae*, Sample Rash1-7, Zone NP17, 19-20. *Reticulofenestra umbilicus*, Sample Rash3-11, Zone NP19/20, 21-22. *Reticulofenestra hillae*, Sample Rash1-6 Zone NP17, 23. *Micrantholithus astrum*, Sample Rash1-11, Zone NP17, 24-25. *Coccolithus pelagicus*, Sample Rash2-6 Zone NP19/20.

regional unconformity that defines the top of the upper Rashrashiyah member at sections Rash2 and Rash3 as a new formation; named as the Qurayyat Formation based on some field observations: i) the lithology of the Qurayyat Formation differs substantially from the underlying Rashrashiyah Formation and the overlying siliciclastic-dominated Sirhan Formation (Figs. 6e-f and 7a-c); ii) the unconformable contact with the underlying and overlying formations can be walked laterally for several hundreds of meters; iii) the Qurayyat Formation is thick enough (15 m to 26 m); and iv) the formation is

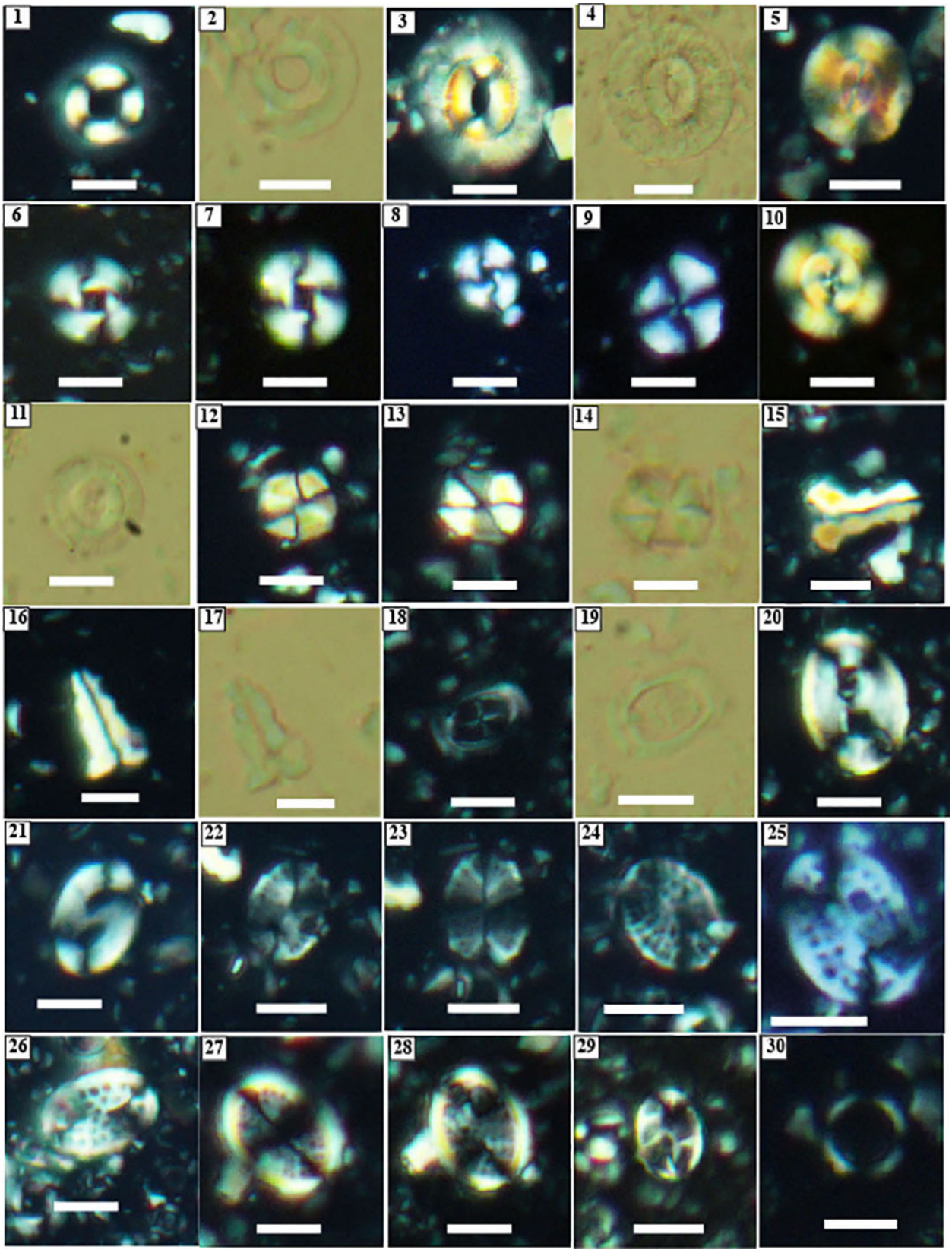

Fig. 3 - Photomicrographs for calcareous nannofossil taxa retrieved from the investigated sections of the Rashrasheyia area, 1-2. Coccolithus formosus, Sample Rash1-6, Zone NP17, 3-4. *Coccolithus eopelagicus*, Sample Rash1-9, Zone NP17, 5. *Reticulofenestra stavensis*, Sample Rash1-2, Zone NP17, 6-8. *Cyclicargolithus floridanus*, Sample Rash3-1, Zone NP19/20, 9. *Cyclicargolithus luminis*, Sample Rash2-13, Zone NP19/20, 10-11. *Reticulofenestra isabellae*, Sample Rash1-73, Zone NP18, 12-14. *Lanternithus minutus*, Sample Rash2-4, Zone NP19/20, 15-17. *Zygrhablithus bijugatus*, Sample Rash3-1, Zone NP19/20, 18-19. *Campylosphaera dela*, Sample Rash-5, Zone NP17, 20. *Pontosphaera duocava*, Sample Rash1-1, Zone NP17, 21. *Pontosphaera exilis*, Sample Rash1-3, Zone NP17, 22-24. *Pontosphaera pectinata*, Sample Rash1-5, Zone NP17, 25-26. *Pontosphaera multipora*, Sample Rash1-2, Zone NP17, 27-28. *Pontosphaera alta*, Sample Rash1-2, NP17 Zone, 29. P*ontosphaera wilsonii*, Sample Rash1-1, Zone NP17. 30. *Coronocyclus nitescens*, Sample Rash1-25, Zone NP17.

mappable across the area of study. Accordingly, the description of the Qurayyat Formation type sections follows the International Commission on Stratigraphy (ICS) guidelines (Murphy & Salvador 1999).

The southern cliff near the Quarry Region east of the Qurayyat City (Lat. 31° 25.022' N and long. 37° 21.148' E) exhibits the most complete and representative succession of the Qurayyat Formation and is proposed as the type locality. In the type section (Rash3), the Qurayyat Formation attains a thickness of about 26 m. The formation consists at the base of 0.8 to 1 m thick grey, massive, and densely bioturbated fossiliferous limestone with an irregular erosional base mantled with reworked molluscan shells (Fig. 3b-d). It is characterized by a marker bed that extends for several hundred meters along strike. The maker bed is overlain by a sharp-based, white to light grey, thick-bedded massive limestone (about 4 m thick) containing yellowish brown nodules and bioturbated by vertical burrows at the top. This portion of the unit is overlain by two marl-limestone cycles, 3.5 and 4.5 m thick, respectively. Each cycle starts at the base with relatively thick marl (about 2.5 m thick) and ends with thick massive white limestone bioturbated by vertical burrows at the top (Fig. 7e, f). The upper 10 m of the Qurayyat Formation consists of thick-bedded, white, hard, coarse-grained limestone, locally fossiliferous with echinoid shell fragments and burrowed by *Thalassinoides* trace fossils. The limestone at the top becomes sandy and contains disseminated chert nodules. An unconformable contact defined by thick basal conglomerate separates the Qurayyat Formation below from the Sirhan Formation above.

Calcareous nannofossils biostratigraphy

The strata of the Rashrashiyah Formation contain moderately to well-preserved calcareous nannofossil assemblages, allowing reliable identification of key biostratigraphic marker species. It is noteworthy that calcareous nannofossil preservation varies throughout the studied succession and reflects changes in depositional conditions. The Middle to Upper Eocene interval is characterized by generally well-preserved assemblages, with coccoliths showing clear morphological features and limited evidence of dissolution or overgrowth, indicating favorable pelagic carbonate sedimentation under relatively stable marine conditions. In contrast, the Oligocene interval exhibits predominantly moderate to poor preservation, marked by partial dissolution and fragmentation. This decline in preservation quality coincides with increased detrital input, suggesting enhanced terrigenous influx and dilution of carbonate sediments, which likely influenced both preservation potential and assemblage composition. Accordingly, the zonal assignment was difficult for the sediments of the Qurayyat Formation because of scarcity and poor preservation.

A total of 85 calcareous nannofossil species belonging to 26 genera were identified in the studied succession, indicating a relatively diverse assemblage across the investigated interval. Biostratigraphic events and the distribution patterns of the most significant species discussed below cover the interval from the Middle Eocene Zone NP17 to the Early Oligocene Zone NP21. These findings are also compared with results from other localities (Fig. 8), supporting the reliability of the established zonation and facilitating regional stratigraphic comparison.

Discoaster saipanensis Zone (NP17)

The Bartonian *Discoaster saipanensis* Zone NP17 is the oldest recognized biozone in the study area. It is identified from the lower and middle members of the Rashrashiyah Formation in samples spanning from Rash1-1 to Rash1-69, encompassing approximately 33.5 m thick (Fig. 9). The recognition of the top Zone NP17 is primarily constrained by the lowest occurrence (LO) of *Chiasmolithus oamaruensis* (Martini 1971), which coincides with the base of Subzone CP15a in the zonal scheme of Okada and Bukry (1980), and CNE15-CNE17, as well as the lower part of Zone CNE18 of Agnini et al. (2014). This interval is characterized by a highly diverse and abundant nannofossil assemblage, including *Ch. grandis*, *F. obtusus*, *Campylosphaera dela*, *Pontosphaera wilsonii*, *Helicosphaera clarissima*, *Sphenolithus pseudoradians*, *Reticulofenestra daviesii*, *Neochiastozygus tenansa*, *Coccolithus biparteoperculatus*, *Micrantholithus astrum*, *Calcidiscus bicircus*, *Pontosphaera latoculata*, and *Pontosphaera pectinata* (see Appendix 2).

In the present study, *Ch. oamaruensis* is recorded as rarely occurring. However, the occurrence of *Chiasmolithus grandis* and the absence of *Chiasmolithus solitus* assign this interval to Zone NP17. Consequently, the top of this zone is locally delineated and approximated based on the highest occurrence

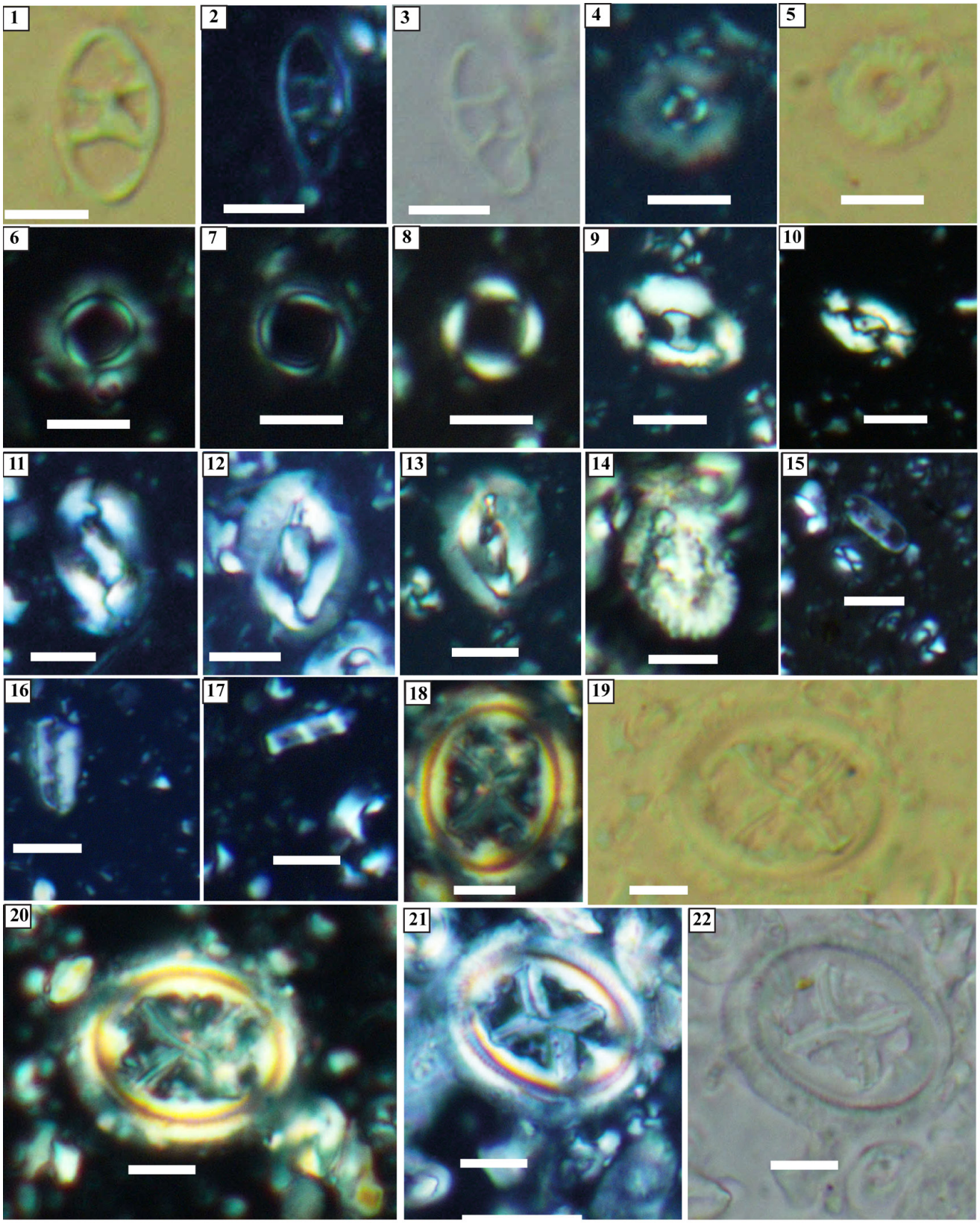

Fig. 4 - Photomicrographs for calcareous nannofossil taxa retrieved from the investigated sections of the Rashrasheyia area, 1. *Neococcolithes dubius*, Sample Rash1-2, Zone NP17, 2-3. *Neococcolithes minutus*, Sample Rash1-56, Zone NP17, 4-5. *Markalius inversus*, Sample Rash1-3, Zone NP17, 6. *Umbilicosphaera protoannulus*, Sample Rash1-1, Zone NP17, 7. *Umbilicosphaera bramlettei*, Sample Rash1-8, Zone NP17, 8. *Umbilicosphaera jordanii*, Sample Rash1-9, Zone NP17, 9-10. *Helicosphaera bramlettei*, Sample Rash1-10, Zone NP17, 11. *Helicosphaera euphratis*, Sample Rash1-4, NP17 Zone, 12-13. *Helicosphaera clarissima*, Sample Rash3-4, Zone NP19/20, 14. *Helicosphaera reticulata*, Sample Rash1-4, Zone NP17, 15-17. *Isthmolithus recurvus*, 15-16 planar view, 17- side view, Sample Rash2-8, Zone NP19/20, 18-20. *Chiasmolithus grandis*, Sample Rash1-63, Zone NP17, 21-22. *Chiasmolithus grandis*, Sample Rash1-2, Zone NP17.

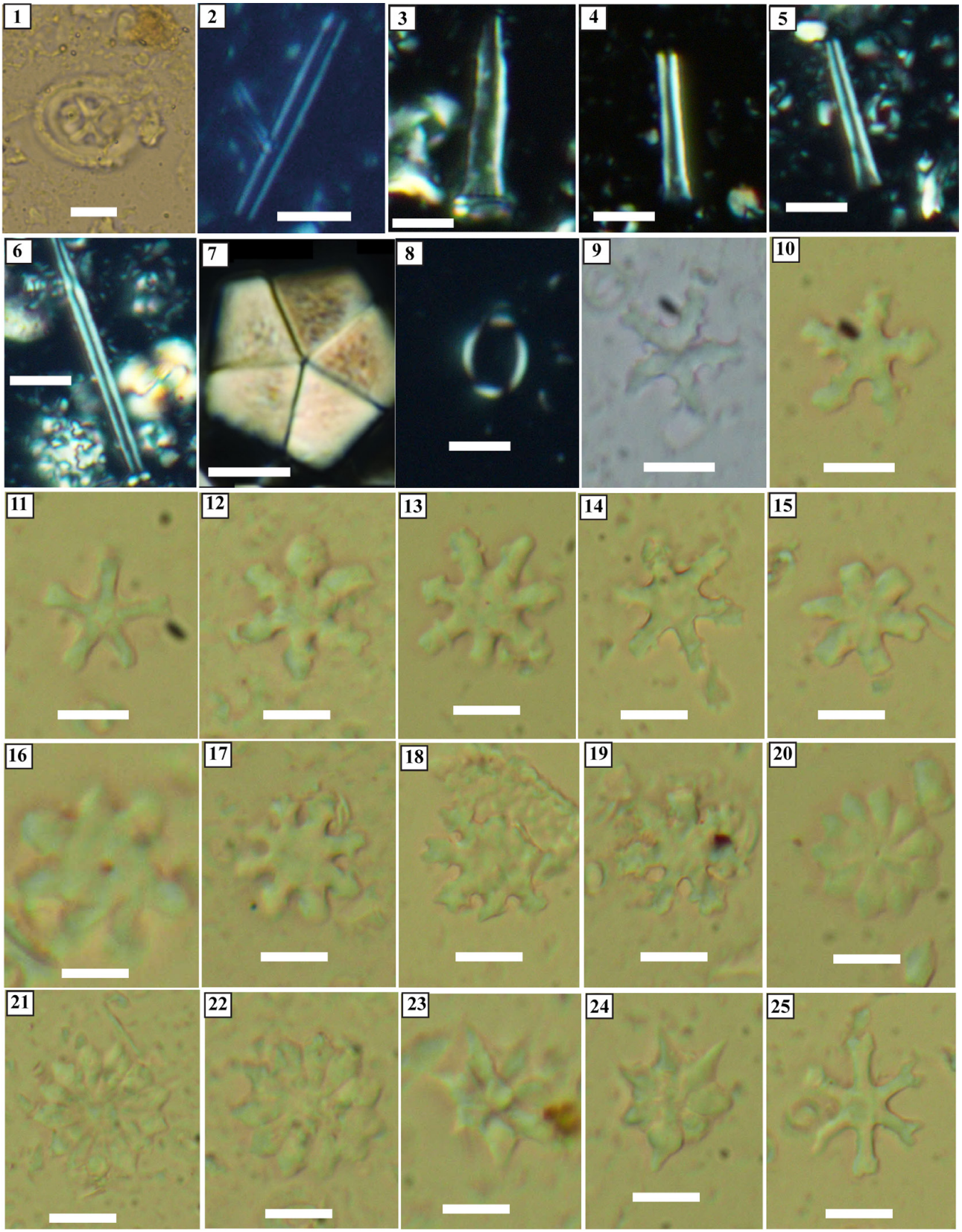

Fig. 5 - Photomicrographs for calcareous nannofossil taxa retrieved from the investigated sections of the Rashrasheyia area, 1. *Chiasmolithus oamaruensis*, Sample Rash1-81, Zone NP19/20. 2-3. *Blackites spinosus*, Sample Rash2-13, Zone NP19/20. 4-5. *Blackites stilus*, Sample Rash2-7, Zone NP19/20, 6. *Blackites tenuis*, Sample Rash3-11, Zone NP19/20, 7. *Braarudosphaera bigelowii*, Sample Rash2-3, Zone NP19/20. 8. *Syracosphaera tanzanensis*, Sample Rash2-3, Zone NP19/20, 9-11. *Discoaster tanii*, Sample Rash2-8, Zone NP19/20, 12-15. *Discoaster nodifer*, Sample Rash2-4, Zone NP19/20, 16-19. *Discoaster binodosus*, Sample Rash1-11, Zone NP17, 20-22. *Discoaster barbadiensis*, Sample Rash1-8, Zone NP17. 23-24. *Discoaster saipanensis*, Sample Rash3-3, Zone NP19/20, 25. *Discoaster deflandrei*, Sample Rash1-3, Zone NP17.

(HO) of *Ch. grandis* (Ghandour et al. 2023, Messaoud et al. 2023) and further constrained by the common occurrence of *Reticulofenestra erbae* (Agnini et al. 2014). Furthermore, the co-occurrence of the *Furcatolithus obtusus* and *Reticulofenestra bisecta* in the investigated samples supports correlation with Zone CNE15 (Agnini et al. 2014). Similarly, in the Arabian Plate, the nominated nannofossil zone has been recorded from eastern Jordan with ~ 4 m thick (Farouk et al. 2015) based on the lowest occurrence of *Ch. oamaruensis*, whereas, to the west of this study in Jordan, the NP17 Zone was not recorded (Farouk et al. 2013). On the other hand, in the Zagros Basin of Iran, Senemari (2021) reported the NP17 Zone based on the acme occurrence of *R. erbae*, and attaining ~15 m.

Chiasmolithus oamaruensis Zone (NP18)

The base of this zone defines the Bartonian/Priabonian boundary (Bukry 1975). In the present study, the base of Zone NP18 is established by the concurrent bioevents marked by the LO of *Chiasmolithus oamaruensis* and the HO of *Chiasmolithus grandis*, whereas the top is defined by the LO of *Isthmolithus recurvus*. This zone was recorded exclusively from section Rash1, where it attains a thickness of approximately 5 m (Fig. 9). The interval is characterized by a moderately to highly abundant and diverse nannofossil assemblage, including *Reticulofenestra erbae*, *R. isabellae*, *R. hillae*, *Markalius inversus*, and *Syracosphaera tanzanensis* (see Appendix 2).

The base of this zone coincides with the Subzone CP15a zonal boundary in the zonation of Okada and Bukry (1980). This zone is equivalent to the middle part of the Zone CNE18 (Agnini et al. 2014). Noteworthy that both *Chiasmolithus* and *Isthmolithus* are generally rare to absent in low latitudes, making Zone NP18 difficult to distinguish in these regions. Conversely, they are more common in mid- to high-latitudes, where the identification of this zone is straightforward (Perch-Nielsen 1985). Aubry (1984) documented their scarcity in tropical–subtropical assemblages and noted their greater abundance at higher latitudes. Similarly, Agnini et al. (2014) emphasized that events involving *Chiasmolithus* and *Isthmolithus* are challenging to detect in low-latitude sections due to their rarity. However, Farouk et al. (2015) recorded a 22 m thick layer of massive limestones alternating upward to chalk with nodular chert in parts, encompassing the Zone NP18 in northern Jordan, based on the LO of *I. recurvus*, and was absent from the southeastern border between Jordan and Saudi Arabia (Farouk et al. 2013). Additionally, Senemari (2021) documented 30 m thick marly-dominated beds covering the nominated zone in the Zagros Basin of Iran, using the LO of *I. recurvus*.

Isthmolithus recurvus/Sphenolithus pseudoradians (Zone NP19/NP20)

The LO of *Isthmolithus recurvus* marks the base of both CP15b (Okada & Bukry 1980) and zones NP19/20 (Martini 1970). The combined zone is equivalent to the upper part of Zone CNE18, and zones CNE19-CNE20 as defined by Agnini et al. (2014). Although Martini (1971) originally designated the LO of *Sphenolithus pseudoradians* as the base of Zone NP20, subsequent studies (Perch-Nielsen 1985, Dunkley Jones et al. 2008, Bergen et al. 2017) demonstrated that *S. pseudoradians* is long-ranging (extending down into NP15–NP16), morphologically similar to *S. radians*, and often rare or absent in many stratigraphic sections. Consequently, NP19 and NP20 cannot be clearly separated, and many researchers combine them or use alternative markers such as the LO/LCO of *I. recurvus* or *Discoaster saipanensis* HOs for regional correlation. Therefore, the interval below the HO of *D. saipanensis*, which defines the Top of Zone NP20/CP15b and consequently the base of Zone NP21 and Subzone CP16a, can be treated as the NP19/NP20 combined zone, equivalent to Subzone CP15b. In the present work, *I. recurvus* was identified in the investigated successions, allowing recognition of the lower boundary of Zone NP19. However, the base of Zone NP20 could not be defined based on the LO of *S. pseudoradians* because this species first appears in Zone NP17 within the investigated sediment samples. The combined Zone NP19/NP20 is recorded in the three sections studied. Scarce specimens of *Isthmolithus recurvus* (plane views) first occur in sample Rash1-79 and persist up to Rash1-84, representing an interval approximately 4 m thick (Fig. 9). Accordingly, the interval between samples Rash1-79 and Rash1-84 is assigned to the *Isthmolithus recurvus* Zone (NP19/20). In section Rash2, the lower part up to the unconformable contact between the Rashrashiyah and Qurayyat formations yielded NP19/20 assemblages, spanning samples Rash2-1 to Rash2-22 and attaining a thickness of 10.8 m (see

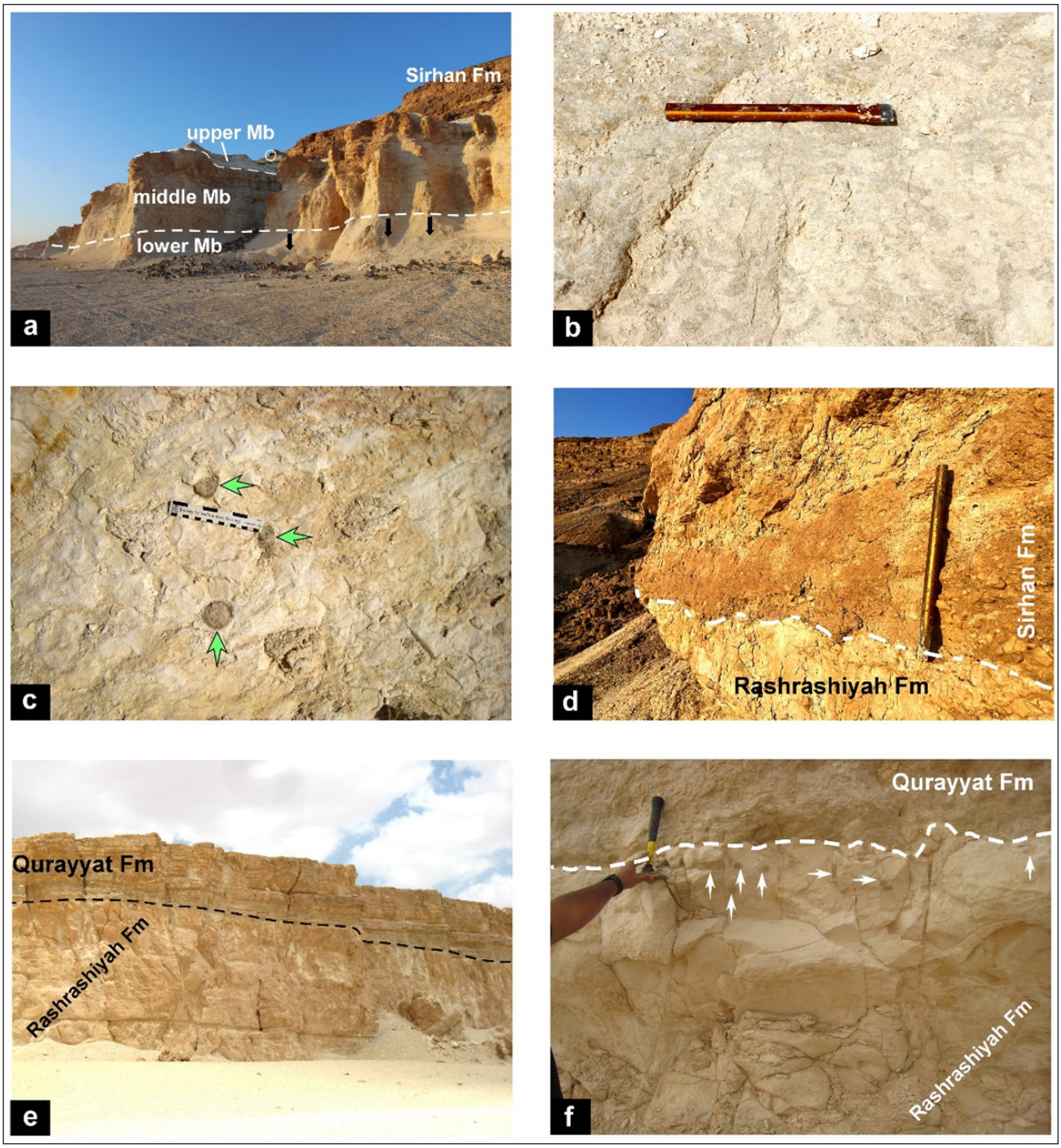

Fig. 6 - Field photographs showing lithostratigraphic framework of Paleogene deposits and their diagnostic features in Rash1 and Rash2 sections. a) Informal subdivision of the Rashrashiyah Formation. Black arrows point to the densely burrowed interval within the lower member. b) *Thalassinoides* trace fossils within the lower member of the Rashrashiyah Formation. c) Barite nodules with different forms and sizes (green arrows) in the middle member of the Rashrashiyah Formation. d) Unconformable contact between the Upper Eocene Rashrashiyah Formation and the Miocene Sirhan Formation. e) Lithostratigraphic subdivision of section Rash2 and the diagnostic lithological features of the upper member of the Rashrashiyah Formation. f) The sharp erosional discontinuity between the Rashrashiyah and Qurayyat formations, white arrows show burrowing of *Glossifungites* ichnofacies at the unconformity surface.

Appendix 3). In section Rash3, the Zone NP19/20 Zone was identified in samples Rash3-1 through Rash3-22, encompassing an approximately 11 m-thick interval (see Appendix 4). Within this zone, calcareous nannofossil assemblages are abundant, diverse, and well-preserved. The characteristic assemblage is dominated by Late Eocene taxa, including *I. recurvus*, *Discoaster saipanensis*, *D. barbadiensis*, *D. tanii*, *D. nodifer*, *Blackites tenuis*, *S. pseudoradians*, *Blackites perlongus*, *Helicosphaera euphratis*, *Umbilicosphaera jordanii*, *U. bramlettei*, and *U. protoannulus* (see Appendices 2-4).

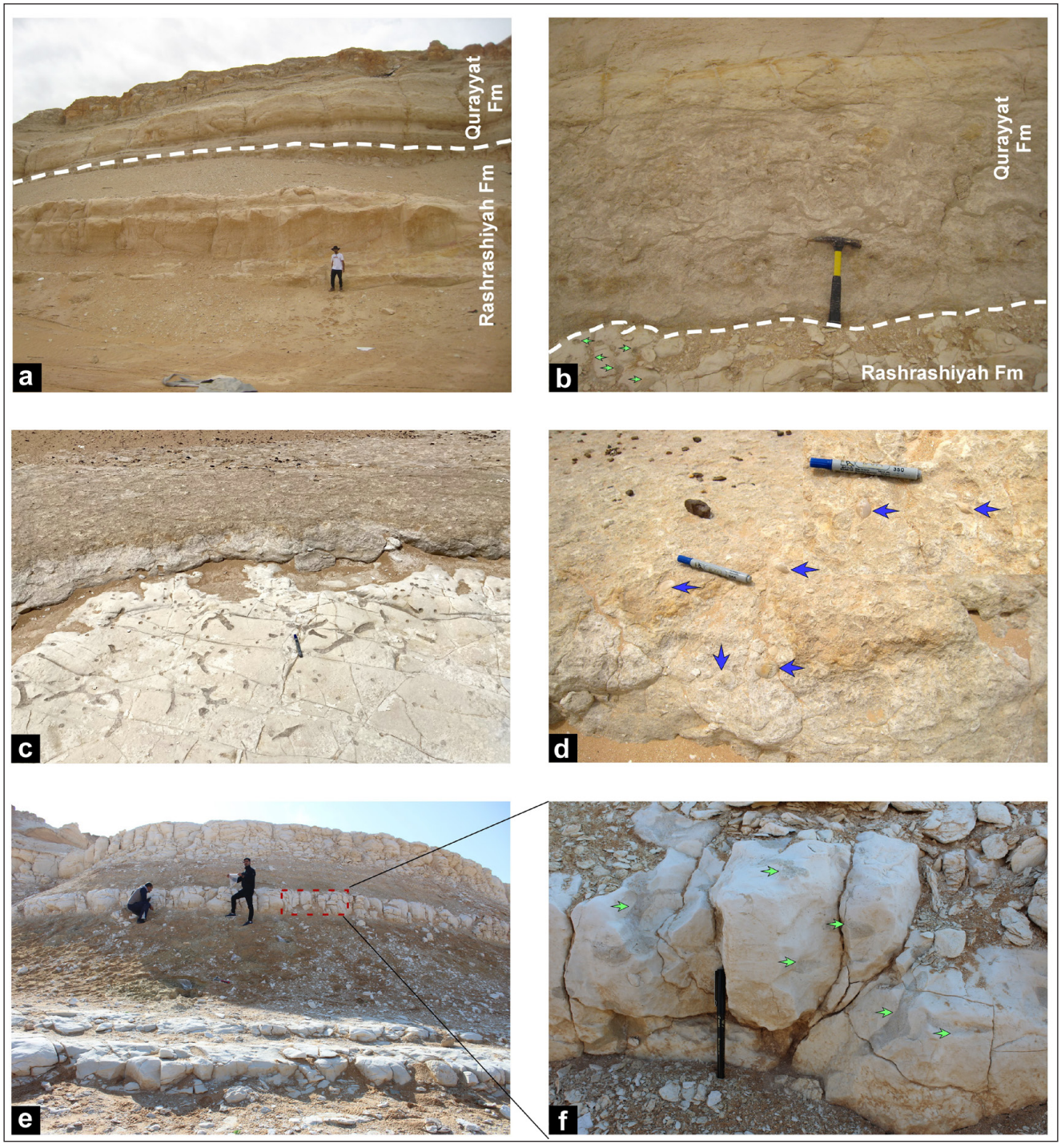

Fig. 7 - Field photographs showing lithostratigraphic framework (a) of Paleogene deposits and their diagnostic features in Rash3. b and c) the sharp erosional disconformity between the Rashrashiyah and Qurayyat formations showing *Thalassinoides* trace fossils defining the unconformity d) Transgressive lag with abundant molluscan shells and shell fragments (blue arrows) immediately above the unconformity surface. e and f) calcareous mudstone to hard limestone cycles in the lower part of the Qurayyat Formation. The top of limestone is burrowed by vertical burrows (green arrows).

The nominated zone (NP19/20) has not been recorded from the surrounding region to the investigated area, particularly Jordan (Farouk et al. 2013; Farouk et al. 2015):D. However, both NP19 and NP20 have been documented in the Zagros Basin of Iran and discriminated and differentiated based on the *S. pseudoradians* (Senemari 2021), whereas Senemari and Jalil (2021) combined the two zones NP19/20 due to the absence of the *S. pseudoradians*.

Ericsonia subdisticha Zone (NP21)

The *Ericsonia subdisticha* Zone (NP21) is de-

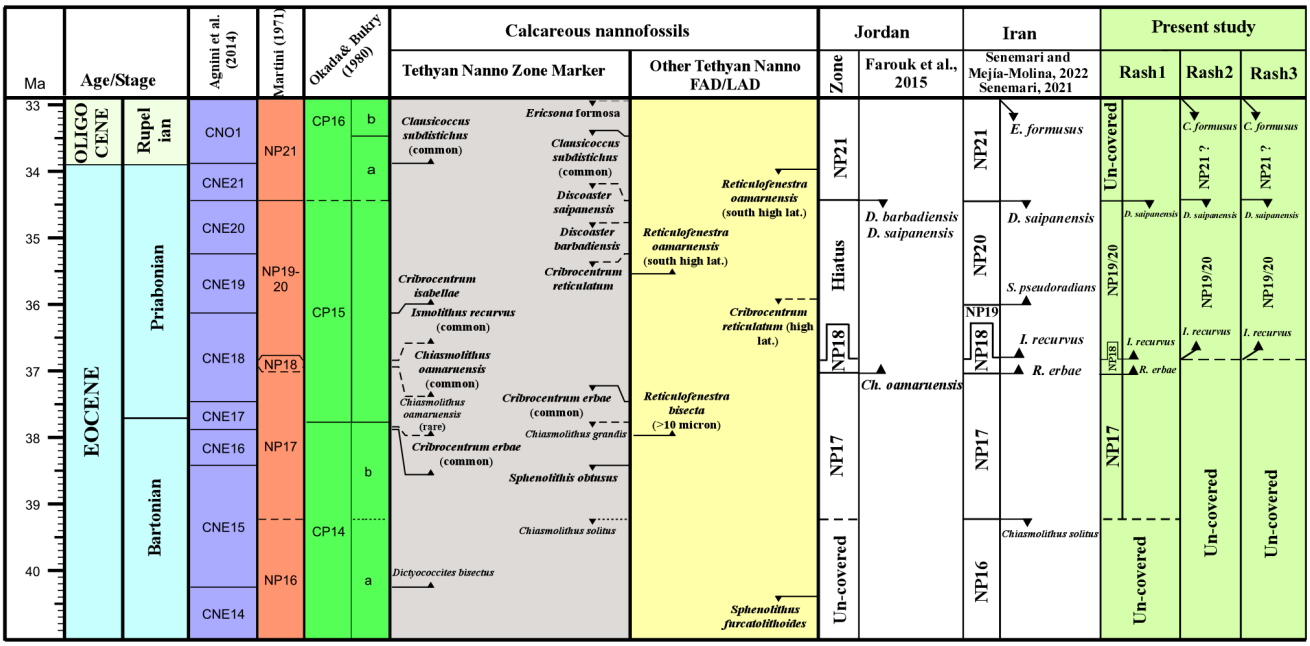

Fig. 8 - Correlation of bioevents and zonations in the present study and different authors spanning the Middle/Upper Eocene to Oligocene boundary.

fined as an interval from the HO of *Discoaster saipanensis* to the HO of *Coccolithus formosus* (Martini 1971). It corresponds to the upper portion of subzones CP16a and CP16b subzones (Okada & Bukry 1980) and is equivalent to zones CNE21/CNO1 of Agnini et al. (2014). This zone was recorded from sections Rash2 and Rash3, encompassing 13 m and 23 m thick limestones with sandy limestone interbedded by shale beds in the Rash 2 section, respectively (see Appendices 3-4). It is noteworthy that both the base and the top of this zone coincide with unconformable contacts, specifically between the upper member of the Rashrashiyah Formation and the Qurayyat Formation at the base, and between the Qurayyat Formation and the Sirhan Formation at the top. The most significant nannofossil taxa within Zone NP21 include *Coccolithus pelagicus*, *C. formosus*, *Cyclicargolithus floridanus*, *R. bisectus*, *R. dictyoda*, *R. umbilicus*, *Sphenolithus moriformis* and *Clausicoccus subdistichus*.

In the present study, the stratigraphic framework of this interval strongly suggests the presence of a depositional hiatus at its base. This is supported by the recognition of an unconformable contact, together with biostratigraphic evidence derived from calcareous nannofossils. Notably, the absence of the characteristic acme of *Clausicoccus subdisticus*, and consequently the lack of a substantial portion of Zone CNO1—whose base approximates the onset of the Oligocene—indicates that part of the earliest Oligocene record is missing. The combined stratigraphic and micropaleontological evidence therefore points to a significant stratigraphic discontinuity separating the Rashrashiyah and Qurayyat formations. Furthermore, this zone corresponds to a low-diversity, low-abundance interval attributed to elevated sediment supply, as evidenced by the poor preservation of nannofossil assemblages. The top of this interval is delineated at the HO of *D. saipanensis*. It is noteworthy that the extinction of the tropical warm-water nannofossil *D. saipanensis* defines the base of the nannofossil Zone NP21 (Martini 1971) and Zone CNE21 (Agnini et al. 2014), representing the earliest documented biotic response to the Late Eocene cooling event. On the Geological Timescale 2012 (GTS2012; Gradstein et al. 2012), the extinction of *D. saipanensis* is dated at 34.44 Ma, preceding the EOB is dated at 33.9 Ma. Notably, a thick layer of limestones and sandstones encompassing the Zone NP21 was recorded in eastern Jordan, as described by Farouk et al. (2013, 2015). They reported a shallowing-up of facies dominated by nummulites, echinoids, and bivalve shells along this zone. Furthermore, in the Zagros Basin, East Tethys, Senemari and Jalili (2021) placed the base of Zone NP21 at the extinction of *D. saipanensis* in the Bid-Zard section southwest of Izeh (Senemari & Mahanipour 2023).

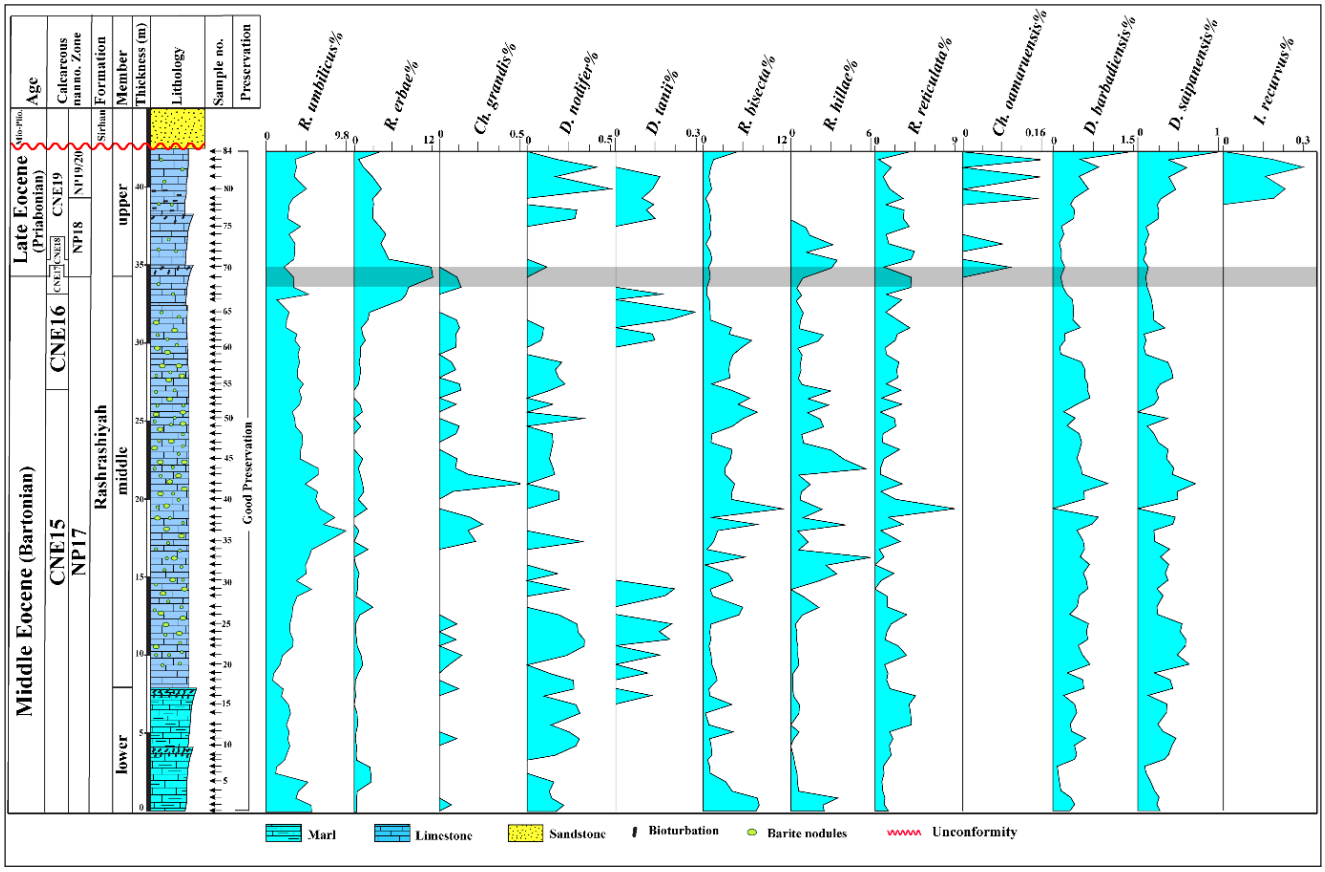

Fig. 9 - Vertical distribution patterns for the marker and dominant calcareous nannofossil retrieved from the investigated Rash1 succession. Note: the shaded grey band marks the Bartonian/Priabonian boundary.

Vertical distribution patterns of calcareous nannofossil assemblages

The Middle–Upper Eocene successions of the Rash1–Rash3 sections display systematic variations in calcareous nannofossil relative abundances that provide robust constraints on assemblage evolution and zonal interpretation under generally good preservation conditions (Figs. 9-11). In Rash1 (Fig. 9), reticulofenestrids dominate the assemblage, with *R. erbae* showing a pronounced acme in the upper part of Zone NP17 (~12%), followed by a gradual decline upward, marking a significant ecological turnover. *R. bisecta* and *R. umbilicus* constitute persistent background taxa (mean values; 3%, and 3.8%, respectively), the former exhibiting episodic proliferation phases and the latter maintaining consistently moderate abundances throughout the interval. *R. reticulata* and *R. hillae* occur steadily at low to moderate frequencies (mean values; 2%, and 1.2%, respectively), reflecting fluctuating paleoenvironmental conditions rather than discrete acme events. *Discoaster* taxa (*D. tanii*, *D. nodifer*, *D. barbadiensis*, and *D. saipanensis*) remain subordinate and show an overall upward decline, consistent with late Eocene cooling trends. The rare but distinct appearances of *Ch. grandis* and *Ch. oamaruensis* further pinpoint the Middle–Late Eocene transition. The first consistent occurrence and subsequent increase of *Isthmolithus recurvus* mark a decisive assemblage turnover at the top of NP18 and the base of the NP19/20 interval, providing a reliable biostratigraphic datum.

In Rash2 and Rash3 (Figs. 10-11), assemblages remain dominated by reticulofenestrids and placolith taxa, particularly *R. umbilicus*, *R. bisecta*, and *Coccolithus* species, whereas *Discoaster* representatives occur only sporadically and in minor proportions. Rash2 exhibits pronounced relative abundance fluctuations in *R. erbae*, including a distinct peak phase prior to the end of the upper Rashrashyiah Formation, alongside a steady upward increase in *R. umbilicus*. *Coccolithus pelagicus* and *C. formosus* display relatively stable but high abundances (mean values; 10.2%, and 9.1%, respectively) prior to their disappearance toward the upper Oligocene interval. In Rash3, *R. bisecta* (mean value; 14.8%) becomes the

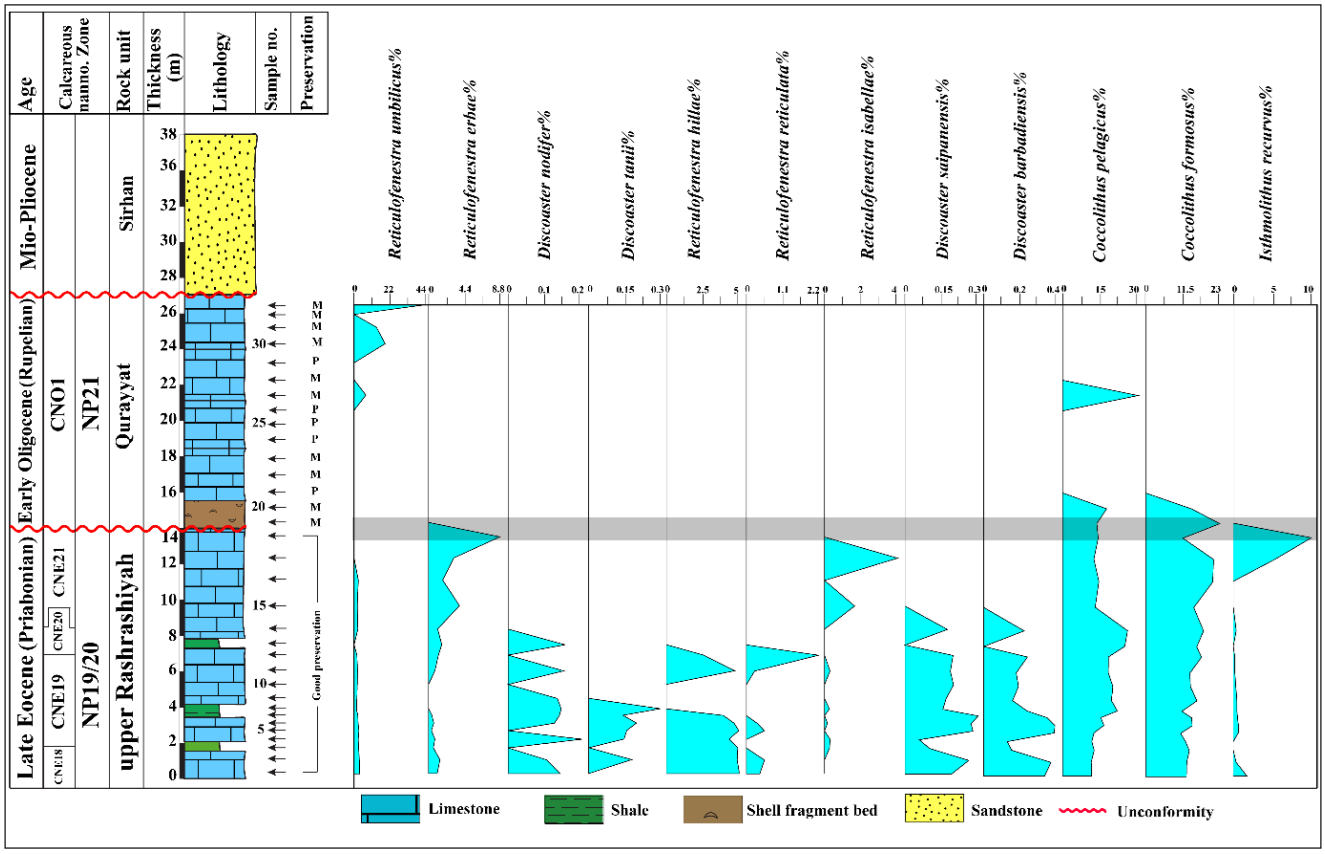

Fig. 10 - Vertical distribution patterns for the marker and dominant calcareous nannofossil retrieved from the investigated Rash2 succession. Note: the shaded grey band marks the Priabonian/Rupelian transition.

dominant taxon, accompanied by moderate contributions from *R. umbilicus* (mean value; 2%) and continuous occurrences of *Coccolithus* taxa (mean value; 26.2%), whereas *R. hillae*, *R. reticulata*, and *R. isabellae* remain subordinate. *Discoaster* species persist at low frequencies, and *Isthmolithus recurvus* occurs sporadically with declining upward abundances. The consistent preservation quality across all sections indicates that these quantitative abundance patterns primarily reflect primary ecological and biostratigraphic signals rather than diagenetic overprinting, thereby supporting the reliability of the inferred Middle–Upper Eocene to Lower Oligocene stratigraphic framework.

Discussion

Based on newly acquired calcareous nannofossil biostratigraphic data, detailed field investigation, and a critical review of published literature, this study proposes a revised stratigraphic scheme for the Paleogene succession in NW Saudi Arabia. The proposed scheme differs significantly from the original stratigraphic interpretation by Meissner et al. (1989). The study of Meissner et al. (1989) lacked precise chronostratigraphic markers and did not adequately consider the role of local tectonics in controlling spatial and temporal stratal deposition and distribution.

Recent studies conducted in Jordan (Farouk et al. 2013; Farouk et al. 2015) and northwestern and southwestern Iraq (Al-Rubai & Al-Mutwali 2020; Al-Mutwali & Al-Rubai 2021) indicated that the Paleogene stratigraphic succession in these regions exhibits remarkable similarities to those observed in the Rashrashiyah area. This correlation suggests that these areas were part of a broadly interconnected carbonate platform, albeit with localized variations in depositional environments.

In contrast to the earlier interpretation, sediments previously assigned to the Rashrashiyah Formation of Middle–Late Eocene age (Meissner et al. 1989) are herein subdivided into two distinct formations: the Middle–Upper Eocene Rashrashiyah Formation, unconformably overlain by the Lower

Oligocene Qurayyat Formation. Furthermore, the Rashrashiyah Formation is informally divided into three members—lower, middle, and upper—based on lithological and biostratigraphic criteria.

Significant lateral facies and age variations are observed in the northern sector of the study area, particularly in sections Rash1 and Rash2. At section Rash1, the three members of the Rashrashiyah Formation (Middle–Upper Eocene) are well exposed and unconformably underlie the siliciclastic-dominated Sirhan Formation. Conversely, section Rash2 begins with the upper member (Upper Eocene) of the Rashrashiyah Formation, which is unconformably overlain by the Qurayyat Formation and, in turn, by the Sirhan Formation. The preservation of the Qurayyat Formation at Rash2 and its absence at Rash1 is interpreted as a consequence of block faulting and differential subsidence across bounding faults. The Rash1 locality, situated on the footwall block, experienced uplift and erosion, leading to the removal or non-deposition of the uppermost Eocene and Oligocene strata. In contrast, Rash2 lies within the downthrown hanging-wall block, which underwent greater subsidence, thereby preserving an incomplete succession of upper Eocene and lower Oligocene strata.

Calcareous nannofossil bioevents and biostratigraphic implications

The LO of *Reticulofenestra isabellae* is consistently documented in the latest Eocene (Priabonian) of the Tethys realm at approximately 36.13 Ma (Agnini et al. 2014). This datum lies within Zone NP19/20 (Martini 1971), CP15 (Okada & Bukry 1980), and CNE18–CNE20 (Agnini et al. 2014), defining the base of CNE19. Regional Neo-Tethyan records, including the Pabdeh Formation (Iran), corroborate its Priabonian occurrence despite local diachroneity (Senemari 2021), while assemblages from the Arabian Plate likewise report its presence in Upper Eocene successions (Aljahdali et al., 2020). In the present study, the LO of *R. isabellae* is employed as an auxiliary biohorizon together with *Reticulofenestra erbae* and *Chiasmolithus grandis* to constrain the onset of Upper Eocene sedimentation.

The stratigraphic significance of *R. erbae* is further supported by its acme event near the Bartonian–Priabonian boundary (~37.46 Ma; Pälike et al. 2006), a phenomenon widely recognized across Tethyan and Indian Ocean sections (Agnini et al. 2011; Fornaciari et al. 2010; Fioroni et al. 2015; Messaoude et al. 2023) and calibrated using associated bioevents such as the HO of *Ch. grandis* and LO of *Ch. oamaruensis* (Agnini et al. 2021). The HO of *Ch. grandis*, which approximates the top of Zone NP17, has historically been used as a zonal biohorizon (Martini 1971; Bukry 1973; Okada & Bukry 1980; Backman 1986), and is treated cautiously due to documented diachroneity and preservation bias (Aubry 1995; Fornaciari et al. 2007; Agnini et al. 2014). Nevertheless, in the present study, the highest occurrence of *Ch. grandis* is at the top of Zone NP17, supported by the topmost common occurrence of the primary marker species *R. erbae* used to detect the top of CNE17 (Agnini et al. 2014). Additional bioevents further refine the Upper Eocene–Lower Oligocene framework. The LO of *Chiasmolithus oamaruensis,* which defines the base of Zone NP18 and CP15a (Martini 1971; Okada & Bukry 1980), although its rarity in low-latitude settings is well documented (Wei & Wise 1989; Bown & Dunkley Jones 2012), whereas its HO (~33.7 Ma) represents a globally calibrated marker for the top of NP19/20 (Backman 1986; Aubry 1995; Gradstein et al. 2020). The LO of *Isthmolithus recurvus* indicates proximity to the NP18–NP19/20 transition and Subzone CP15b (Fornaciari et al. 2010; Agnini et al. 2011), which is consistent with observations from Egypt and Iran (Strougo et al. 2013; Abu Shama 2022; Senemari 2021).

The stratigraphic range of *Reticulofenestra hillae* (NP17–NP22) provides an additional constraint across the Eocene–Oligocene transition, with its HO dated to ~32.02–32.92 Ma (Bown & Dunkley Jones 2012; Arreguín-Rodríguez et al. 2021) and regionally documented within the Rashrashiyah Formation. Finally, the HO of *Discoaster saipanensis*, a widely recognized datum approximating the NP20/NP21 boundary (Martini 1971; Okada & Bukry 1980), occurs near ~34.4 Ma within Chron C13r and is consistently reported across low- to mid-latitude Tethyan successions despite minor diachroneity (Berggren et al. 1995; Persico & Villa 2004; Villa et al. 2008; Fornaciari et al. 2010; Agnini et al. 2014; Messaoud et al. 2020). In the present study, this extinction marks the uppermost NP19/20 and delineates the transition to Zone NP21, reflecting the decline of warm-water discoasters associated with the paleoceanographic reorganization preceding the Eocene–Oligocene transition.

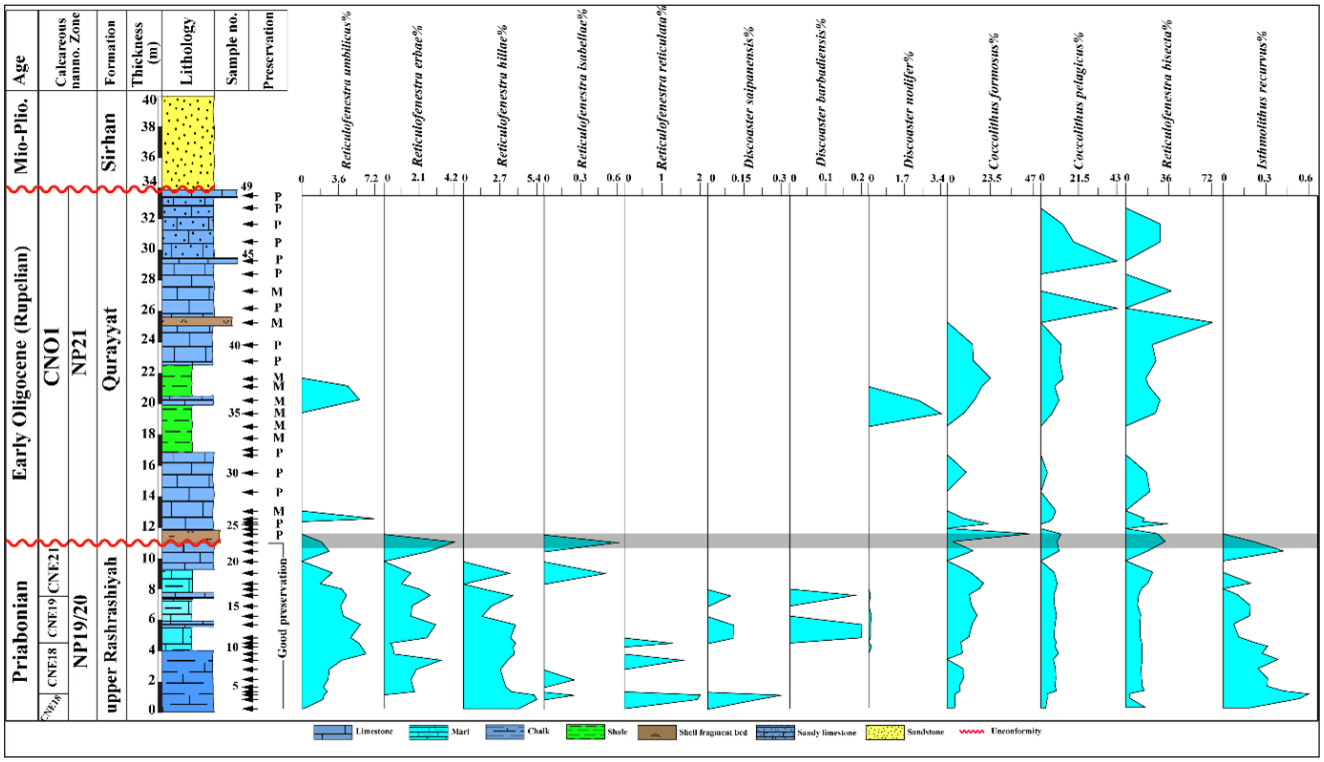

Fig. 11 - Vertical distribution patterns for the marker and dominant calcareous nannofossil retrieved from the type section (Rash3). Note: the shaded grey band marks the Priabonian/Rupelian transition.

Stage Boundaries

Bartonian/Priabonian boundary

The Bartonian/Priabonian boundary is marked by a coherent suite of calcareous nannofossil events that provides one of the most reliable means of correlating Middle and Upper Eocene marine sequences. The transition is positioned near the upper part of NP17, where several well-defined bioevents converge. Among these, the acme of *Reticulofenestra erbae* represents the most distinctive and geographically widespread signal, repeatedly documented in Tethyan, Atlantic, and Indo-Pacific successions (Agnini et al. 2014, Agnini et al. 2017). Closely associated with this horizon is the highest consistent occurrence of *Chiasmolithus grandis*, whose disappearance constitutes a second, globally traceable marker tied to the latest Bartonian NP17 upper biohorizon (Agnini et al. 2021). These events are accompanied by a broader assemblage shift, marked by the decline of large reticulofenestrids and the rise of smaller, more oligotrophic taxa, reflecting the onset of a long-term Late Eocene cooling trajectory (Agnini et al. 2014; Cotton et al. 2017). The Bartonian–Priabonian transition in the Tethyan and peri-Tethyan regions represents one of the most laterally traceable intervals in Cenozoic stratigraphy, owing to its prosperous and relatively stable nannofossil record. Across the southern Tethys, from North Africa through the Levant to the Arabian Plate, this interval is marked by a series of biostratigraphic events that remain broadly synchronous despite differences in sedimentation rate, facies, and platform–basin position (Perch-Nielsen 1985; Aubry 1990; Agnini et al. 2014). In northern Saudi Arabia, where the present study is located, our placement of the Bartonian/Priabonian boundary at the acme occurrence of *Reticulofenestra erbae* and its confirmation by the highest consistent occurrence (HCO) of *Chiasmolithus grandis* accords well with the regional pattern documented across adjacent Tethyan margins.

In Jordan, the Bartonian/Priabonian transition has been delineated using integrated calcareous nannofossil and planktonic foraminiferal biostratigraphy (Farouk et al. 2015). However, the transition could not be precisely defined using nannofossil markers alone; instead, it was constrained by the appearance of large muricate foraminiferal taxa. Although Farouk et al. (2015) identified the top of Zone NP17 based on the LO of *Ch. omaruensis*, they positioned the boundary above this level due to the diachronous nature of *Ch. omaruensis*. Moreover, while the Bartonian/Priabonian boundary is reco-

gnized in eastern Jordan, it is absent in the Wadi El-Ghadaf area west of Qa' Faydat ad Dahikiya (Farouk et al. 2013). In the Tunisian successions, the Bartonian/Priabonian transition has been placed at the top of the Zone CNE16, equivalent to the upper part of NP17 (Messaoud et al. 2023). They delineated the boundary using the common occurrence of *R. erbae* (Agnini et al. 2014). In Iran, the Zagros Basin records the boundary in more heterogeneous facies, yet the same key nannofossil events persist. Studies from the Jahrum, and Pabdeh formations anchor the Bartonian/Priabonian transition at the acme occurrence of the *R. erbae* (Senemari 2021). Within the Arabian Plate, particularly northeastern Saudi Arabia, Korin et al. (2025) demonstrated that the Bartonian/Priabonian boundary is consistently marked by the disappearance of *Ch. grandis* at the zonal NP17/NP18 boundary. The present study fits cleanly within this regional mosaic, where our identification of the Bartonian/Priabonian boundary at the *Reticulofenestra erbae* acme corresponds to a widely reported Tethyan episode of increased abundance of large reticulofenestrids near the top of NP18 Zone. The highest consistent occurrence of *Chiasmolithus grandis* provides a robust secondary marker that aligns precisely with definitions used in Saudi Arabia and Egypt (Abu Shama 2022). The stability of these events across diverse depositional settings reinforces the reliability of nannofossil biostratigraphy for cross-regional correlation and confirms that the northern Arabian Plate preserves a canonical expression of the Bartonian/Priabonian transition.

Priabonian/Rupelian stage

Within the global framework, the Priabonian/Rupelian boundary, marking the EOB, is defined by a significant reorganization of calcareous nannofossil communities, prominently expressed through the terminal decline of several *Discoaster* taxa and the emergence of cold-water–adapted taxa (Agnini et al. 2006). In open-ocean settings, the highest occurrence of *Discoaster saipanensis* represents a robust biomarker located immediately below the EOB cooling pulse and the global extinction of many warm-water discoasters (Persico & Villa 2004; Agnini et al. 2014). This event is widely used to approximate the Priabonian/Rupelian boundary within the upper part of the NP21 Zone (Martini 1971; Perch-Nielsen 1985), particularly in regions influenced by Tethyan circulation. Across the Tethyan and peri-Tethyan realms, the disappearance of *D. saipanensis* is closely associated with a significant reduction in *Discoaster* diversity and the absence, condensation, or extreme thinning of the uppermost Priabonian interval immediately preceding the boundary (Agnini et al. 2014).

In the North African Tethyan margin, including Tunisia and Egypt, the Priabonian–Rupelian boundary is similarly constrained by the HO of *D. saipanensis* along with the disappearance of other warm-water discoasters such as *D. barbadiensis* and *D. tanii* (Bown & Jones 2012). Tunisian successions (e.g., Souar/El-Rahma and other SW Neo-Tethys sections) show a marked reduction in discoasters abundance in upper Priabonian strata, followed by assemblages dominated by reticulofenestrids and smaller placolith taxa (Agnini et al. 2014; Messaoud et al. 2020; Messaoud et al. 2023). Many North African sections also show evidence of a stratigraphic condensation or hiatus across the EOB, commonly attributed to sea-level fall and regional tectonic tilting (Strougo et al. 2013). Likewise, the uppermost Eocene successions in Iran, particularly the Zagros Basin, record the terminal decline of *Discoaster saipanensis* at or just below a pronounced lithological shift and widespread hiatus (Senemari & Jalili 2021). These sediments are frequently bioturbated, rich in echinoid and bivalve debris, and lack both the *C. subdistichus* acme and early Rupelian small-placolith bloom, reinforcing the interpretation of a missing earliest Oligocene interval. Across the Arabian Plate the Priabonian–Rupelian interval is commonly marked by a regionally extensive sequence boundary (base AP11, ~34 Ma) and local hiatuses or condensed sections, features attributed to late Eocene tectonic reorganization of the plate margin and the eustatic sea-level fall associated with Antarctic glaciation (Sharland et al. 2001; Haq & Al-Qahtani 2005; Miller et al. 2005). This pattern is evident in northern Saudi Arabia, where the investigated sections exhibit a well-defined HO of *D. saipanensis*, marking the uppermost part of the Priabonian. Above this event, sedimentological observations, including large-scale bioturbation structures, pervasive burrow networks, and accumulations of bivalves and echinoids, indicate a condensed or disturbed depositional regime consistent with erosion or nondeposition across the EOB. The absence of the characteristic *Clausicoccus subdistichus* acme in our stu-

dy further supports the interpretation that the latest Priabonian and earliest Rupelian intervals are partially or wholly missing.

Eocene/Oligocene Boundary (EOB) in the Arabian Plate

A comprehensive literature review reveals that continuous, chronostratigraphically well-calibrated stratigraphic sections spanning the Eocene-Oligocene are absent across the Arabian Plate. Marine Oligocene strata in the eastern sector of the Arabian Plate are either poorly documented or entirely missing. They have not previously been described in northwestern Saudi Arabia. Recently, Abu-Zied et al. (2025) revised the Paleogene succession in the Rashrashiyah area using planktonic foraminifera and proposed uninterrupted sedimentation across the Eocene/Oligocene boundary (EOB). They placed the EOB at the HO of the planktonic foraminifera *Hantkenina*, which occurs several meters below the unconformity separating the Rashrashiyah and Qurayyat formations. The present study challenges this assumption. Calcareous nannofossil data, combined with regional stratigraphic data, indicate the presence of a major unconformity of variable magnitudes at the EOB throughout the Arabian Plate (Fig. 12). This unconformity equates to the AP10/AP11 sequence boundary of Sharland et al. (2001) and the Zagros Major Hiatus of Lawa and Ghafur (2015) dated to approximately 34 Ma. In the Rashrashiyah area, the EOB is marked by a sharp erosional disconformity separating the Rashrashiyah Formation below from the Qurayyat Formation above (Fig. 12). This disconformity, documented in sections Rash2 and Rash3, exhibits *Glossifungites* ichnofacies and coincides with the extinction of *D. saipanensis* and *D. barbadiensis*. The hiatus likely encompasses the upper part of the *Isthmolithus recurvus* Zone and *Sphenolithus pseudoradians* Zone (NP19/NP20 combined) and the basal to middle portions of Zone NP21. This interpretation is based on both stratigraphic and biostratigraphic evidence. Stratigraphically, the interval coincides with an unconformable contact marking a significant depositional break. Biostratigraphically, several diagnostic taxa and bioevents expected within these zones are absent, most notably the acme of *C subdistichus*, which characterizes a substantial basal part of Zone CNO1 and approximates the base of the Oligocene. Consequently, the absence of the marker species defining the lower and middle NP21 intervals suggests that the sediments corresponding to this time span are missing rather than the result of inhospitable environmental conditions.

Across the Arabian Plate, incomplete stratigraphic sections across the EOB are common (Fig. 12). In Jordan, the lower Oligocene Tayba Formation and its equivalent rest unconformably on Middle Eocene strata, with gaps of 2.1–6.8 Myr (Farouk et al. 2013, Farouk et al. 2015). Similar unconformity occurs in Iraq, where the Palani Formation unconformably overlies the Jaddala Formation in the Sinjar area with a gap of 9-10.5 Myr (Al-Banna et al. 2010; Al-Rubai & Al-Mutwali 2020; Al-Mutwali & Al-Rubai 2021). In Kurdistan, upper Eocene to lower Miocene deposits are entirely absent, where the Middle Miocene Fatha Formation rests unconformably above the Middle Eocene Pila Spi Formation (Lawa & Ghafur 2015). Comparable hiatuses are documented in the main Arabian Basin, the Dammam Dome, Qatar, Kuwait, and Jabal Hafit, UAE (Cherif et al. 1992; Whittle et al. 1996; Weijermars 1999; Al-Saad 2005; Boukhary et al. 2005). In the Dammam Dome, the Lower Eocene Dammam Formation is unconformably overlain by the Lower Miocene Dam/Hadruk Formation with a time gap of approximately 22 Myr (Weijermars 1999). The supra-Dammam unconformity marks a sequence boundary between Tectonomegasequences AP10 and AP11 (Sharland et al. 2001; Al-Husseini 2008). The Dammam Formation is recorded with a reduced thickness or completely eroded from the crest of the dome at Gebel Umm Er-Rus, juxtaposing the Lower Miocene Dam Formation unconformably above the Rus Formation (Weijermars 1999).

Calcareous nannofossils provide a robust basis for high-resolution dating for the Paleogene strata in the Rashrashiyah area. In this study, the extinction of *D. saipanensis and D. barbadiensis* coincides with the erosional disconformity separating the Rashrashiyah and overlying Qurayyat formations. Furthermore, the acme of the *Clausicoccus subdistichus* could not be precisely identified, suggesting that portions of the upper Eocene and lower Oligocene records are missing, and confirming an interruption in sedimentation. Globally, the GSSP for the Rupelian Stage (Lower Oligocene) is defined at Massignano, Italy, with the extinction of *Hantkenina* (Premoli Silva & Jenkins 1993; Bergen et al. 2017). The extinction of *H. alabamensis* is the primary mar-

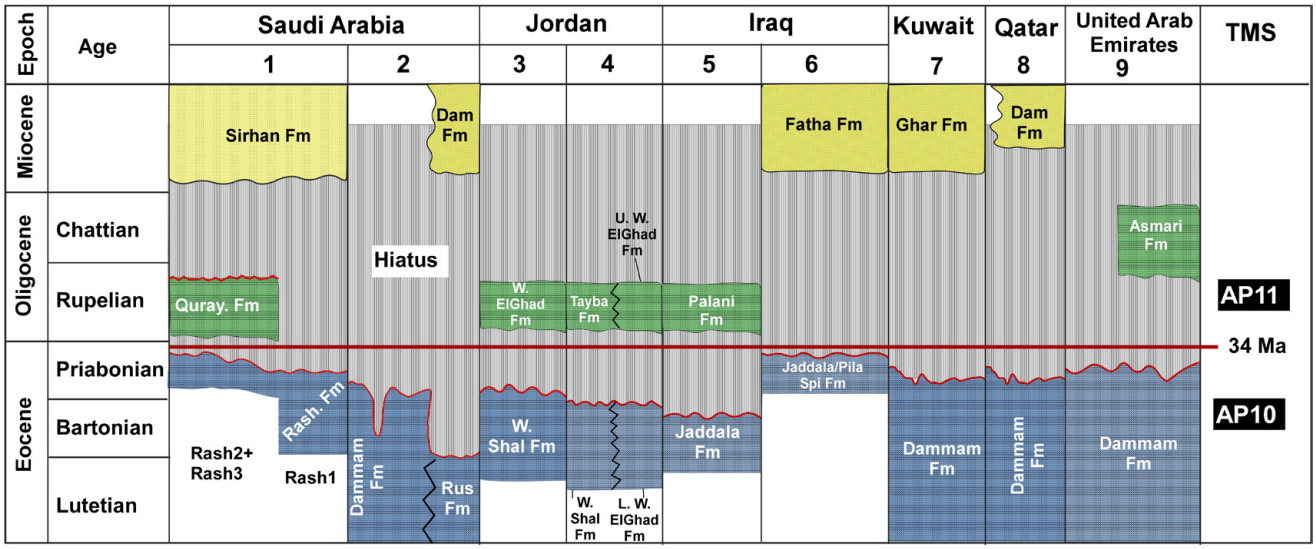

Fig. 12 - Correlation of the stratigraphic framework of Paleogene deposits and the Eocene/Oligocene unconformity of different magnitudes across the Arabian Plate. 1) Present study, 2) Main Arabian Basin (Sharland et al. 2001; Weijermars 1999), 3) SE Jordan, Qa' Faydat ad Adahkiya (Farouk et al. 2015), 4) NW and E Jordan (Farouk et al. 2013), 5) Sinjar basin, NW Iraq (Al-Mutwali & Al-Rubai 2021), 6) Zagros Fold Belt, Kurdistand (Lawa & Ghafur 2015), 7) Kuwait (Sharland et al. 2001; Weijermars 1999), 8) Qatar (Al-Saad 2005), 9) UAE, (Alsharhan & Nairn 1997; Sadooni & Alsharhan 2019), and TMS: Tectono-megasequence of Arabian Plate (Sharland et al. 2001).

ker for worldwide correlation of the EOB. Notably, *D. barbadiensis* and *D. saipanensis* disappear earlier, at ~34.77 Ma and ~34.44 Ma, respectively. This indicates that the extinction of *D. saipanensis* predates 34.4 Ma. In northeastern Tunisia, the acme of *Clausicoccus subdistichus* coincides with the extinction of hantkeninids, a level that defines the EOB (Messaoud et al. 2020).

The disappearance of *Hantkenina* in the study of Abu-Zied et al. (2025) may reflect ecological factors, rendering it an unreliable marker for the EOB in this region. Farouk et al. (2015) recorded *Hantkenina alabamensis* in a single sample from the uppermost part of the Wadi Shallala Formation immediately below the E/O unconformable contact, with *D. barbadiensis* extinct at the unconformable contact and immediately above the extinction level of *H. alabamensis*, whereas *D. saipenensis* disappeared 2 m below the extinction level of *H. alabamensis*.

Conclusions

The carbonate-dominated Paleogene deposits in the Rashrashiyah area, NW Saudi Arabia, are reinterpreted as two formations separated by a regional unconformity. These formations are the Middle-Upper Eocene Rashrashiyah Formation and the newly introduced Lower Oligocene Qurayyat Formation. The spatial distribution of the two formations reflects tectonic control, with block faulting and differential subsidence influencing the stratigraphic preservation of the Qurayyat Formation sediments. The Qurayyat Formation records marine Oligocene deposits for the first time in NW Saudi Arabia. Based on calcareous nannofossil biostratigraphy, the studied deposits are assigned to zones NP17-NP21, spanning the Bartonian–Rupelian interval. The unconformable contact between the two formations is defined by the coincidence with the extinction of *Discoaster saipanensis* and *Discoaster barbadiensis*, which contrasts with earlier interpretations of continuous Eocene sedimentation. The updated stratigraphic framework is consistent with regional trends across the Arabian Plate, where the Eocene-Oligocene transition is associated with a major unconformity of varying magnitude, related to tectonic uplift and eustatic sea-level fall.

Author Contributions. All authors participated directly in the preparation of the article. Mohammed Aljahdali: Supervision, Project administration, Funding acquisition, Conceptualization, sample collection, Methodology, writing, review, and editing. Ibrahim Ghandour: Conceptualization, Field studies and sample collection, Visualization, writing, review, and editing. Mahmoud Faris: Methodology, Investigation, Data analysis, Data Curation, writing, review, and editing. Rashad Bantan: Conceptualization, Data Curation, Resources, review and editing. Mazen Alsaddah: Field studies and sample collection, Methodology, and data analysis. Khalid Alrizqi: Field studies and sample collection, Methodology, and data analysis. Bridget Wade: Writing, review and editing. Ramadan El-Kahawy: Methodology, Investigation, Data analysis, Data Curation, Visualization, writing – review and editing.

Funding. This research work was funded by the Deanship of Scientific Research (DSR) at King Abdulaziz University (KAU), Jeddah, Saudi Arabia, under grant no. (G: 703-150-1443). The authors gratefully acknowledge the technical and financial support provided by the King Abdulaziz University Deanship of Scientific Research, DSR, Jeddah, Saudi Arabia.

Data Availability Statement. The data supporting the results of this research are available upon request. Interested researchers may contact the corresponding author to obtain access

*Acknowledgments***:** This research work was funded by the Deanship of Scientific Research (DSR) at King Abdulaziz University (KAU), Jeddah, Saudi Arabia, under grant no. (G: 703-150-1443). The authors gratefully acknowledge the technical and financial support provided by the King Abdulaziz University Deanship of Scientific Research, DSR, Jeddah, Saudi Arabia. The authors express their deepest gratitude and appreciation to the Royal Highness Prince Faisal bin Nawaf Al Saud, the Prince of Al-Jawf Province, for his support, encouragement, and guidance to the relevant authorities in the region in facilitating all procedures and means, which had a profound impact on achieving the goal of this work. Sincere thanks and gratitude are extended to the leadership of the Border Guard in Al-Jawf Province for their assistance during the fieldwork. Sincere thanks go to Dr. Hamdy Aboulela and Dr. Ramadan Abu Zied (KAU) for their assistance in the fieldwork. The authors are grateful and indebted to Mr. Ahmed S. Alajaj for his hospitality and for providing full accommodation and support during the field trips. The authors gratefully acknowledge Lucia Angiolini (Editor-in-Chief), Silvia Gardin (Section Editor), and the two anonymous reviewers for their constructive comments and valuable suggestions, which significantly improved the manuscript.

References

Abu Shama A.M. (2022) - Calcareous nannofossil biostratigraphy of the Eocene succession in West Central Sinai, Egypt. *Journal of African Earth Sciences,* 194: 104609.

Abu Zied R.H., Aljahdali M.H., Ghandour I.M., Al-Malki A.A. & Bantan R.A. (2025) - Revised lithostratigraphy and planktonic foraminiferal biostratigraphy of upper middle Eocene-lower Oligocene successions from Northern Saudi Arabia. *Arabian Journal of Geosciences,* 18: 233.

Agnini C., Backman J., Boscolo-Galazzo F., Condon D.J., Fornaciari E., Galeotti S., Giusberti L., Grandesso P., Lanci L. & Luciani V. (2021) - Proposal for the global boundary stratotype section and point (GSSP) for the Priabonian stage (Eocene) at the Alano section (Italy). *Episodes Journal of International Geoscience,* 44(2): 151-173.

Agnini C., Fornaciari E., Giusberti L., Grandesso P., Lanci L., Luciani V., Muttoni G., Pälike H., Rio D., Spofforth D.J. & Stefani C. (2011) - Integrated biomagnetostratigraphy of the Alano section (NE Italy): A proposal for defining the middle-late Eocene boundary. *Bulletin*, 123(5-6), 841-872.

Agnini C., Fornaciari E., Raffi I., Catanzariti R., Pälike H., Backman J. & Rio D. (2014) - Biozonation and biochronology of Paleogene calcareous nannofossils from low and middle latitudes." *Newsletters on stratigraphy,* 47(2): 131-181.

Agnini C., Monechi S. & Raffi I. (2017) - Calcareous nannofossil biostratigraphy: historical background and application in Cenozoic chronostratigraphy. *Lethaia,* 50(3): 447-463.

Agnini C., Muttoni G., Kent D.V. & Rio D. (2006) - Eocene biostratigraphy and magnetic stratigraphy from Possagno, Italy: The calcareous nannofossil response to climate variability." *Earth and Planetary Science Letters*, 241(3-4): 815-830.

Ahmed A., Aseri A. & Ali K. (2022) - Geological and geochemical evaluation of phosphorite deposits in northwestern Saudi Arabia as a possible source of trace and rare-earth elements." *Ore Geology Reviews,* 144: 104854.

Arreguín-Rodríguez G.J., Trasviña-Moreno C.A., Thomas E. & Alegret L. (2021) - Updating a Paleogene magnetobiochronological time scale through graphical integration. *MethodsX*, 8, p.101291.

Al-Banna N.Y., Al-Mutwali M.M. & Ismail N.R. (2010) - Oligocene stratigraphy in the Sinjar Basin, northwestern Iraq. *GeoArabia,* 15(4): 17-44.

Al-Hobaib A.S., Baioumy H.M. & Al-Ateeq M.A. (2013) - Geochemistry and origin of the Paleocene phosphorites from the Hazm Al-Jalamid area, northern Saudi Arabia. *Journal of Geochemical Exploration,* 132: 15-25.

Al-Husseini M. (2008) - Launch of the Middle East Geologic Time Scale. *GeoArabia*, 13: 185-188.

Al-Mutwali M. & Al-Rubai H. (2021) - Geological history, Ichnofacies and Sequence Stratigraphy of the Eocene–Oligocene Boundary at Sinjar Area, Northwestern Iraq. *Iraqi National Journal of Earth Science,* 21(1): 27.20-45.20.

Al-Rubai H. & Al-Mutwali M. (2020) - Planktonic Foraminiferal Biosatratigraphy of the Eocene-Oligocene Boundary at Sinjar Area, NW Iraq. *Iraqi National Journal of Earth Science,* 20(2): 1.0-18.10.

Al-Saad H. (2005) - Lithostratigraphy of the Middle Eocene Dammam Formation in Qatar, Arabian Gulf: effects of sea-level fluctuations along a tidal environment. *Journal of Asian Earth Sciences,* 25(5): 781-789.

Aldaajani T.Z., Almalki K.A. & Betts P.G. (2021) - Plume versus slab-pull: Example from the Arabian Plate. *Frontiers in Earth Science,* 9: 700550.

Aljahdali M., Elhag M., Mufrreh Y., Memesh A., Alsoubhi S. & Zalmout I. (2020) - Upper Eocene calcareous nannofossil biostratigraphy: a new preliminary priabonian record from northern Saudi Arabia. *Applied Ecology Environmental Research,* 18(4).

Aljahdali M.H., Wise Jr. S.W., Bord D., Pospichal J. & Cevik T. (2019) - A review of tropical calcareous nannofossil biostratigraphy across the early/late oligocene: a new taxon-range zone; A review of tropical calcareous nannofossil biostratigraphy across the early/late oligocene: a new taxon-range zone. *Newsletters on Stratigraphy,* 52(3): 321-340.

Allam S., Korin A., Herlambang A., Humphrey J.D., Alnajjar M.I., Bahameem A.A., Memesh A.M., Zalmout I. S. & Kaminski M. (2025) - Stable carbon and oxygen isotopes of benthic and planktonic foraminifera as palaeoenvironmental and palaeoclimatic proxies for the Bartonian-Priabonian in northwestern Saudi Arabia. *Geological Quarterly*: 69-26; 10.7306/gq. 1799.

Allen M., Jackson J. & Walker R. (2004) - Late Cenozoic reorganization of the Arabia-Eurasia collision and the comparison of short-term and long-term deformation rates. *Tectonics,* 23(2).

Allen M.B. & Armstrong H.A. (2008) - Arabia-Eurasia collision and the forcing of mid-Cenozoic global cooling. *Palaeogeography, palaeoclimatology, palaeoecology,* 265(1-2): 52-58.

Alsharhan A. & Nairn A. (1995) - Tertiary of the Arabian Gulf: sedimentology and hydrocarbon potential. *Palaeogeography, Palaeoclimatology, Palaeoecology,* 114(2-4): 369-384.

Alsharhan A. & Nairn A. (1997) - Sedimentary basins and petroleum geology of the Middle East, Elsevier.

Aubry M.-P. (1984) - Handbook of Cenozoic Calcareous Nannoplankton: Heliolithae: helicoliths, cribriliths, lopadoliths and others, Micropaleontology Press, American Museum of Natural History.

Aubry M.-P. (1990) - Handbook of Cenozoic calcareous nannoplankton. Book 4: Heliolithae (Helicoliths, Cribriliths, Lopadoliths and others). Micropaleontology Press, American Museum of Natural History.

Aubry M.-P. (1995) - Towards an upper Paleocene-lower Eocene high resolution stratigraphy based on calcareous nannofossil stratigraphy. *Israel Journal of Earth Sciences,* 44: 239-253.

Aubry M.-P. (1999) - Handbook of Cenozoic Calcareous Nannoplankton: Book 5: Heliolithae (Zygoliths and Rhabdoliths), Micropaleontology Press, the American Museum of Natural History.

Backman J. (1986) - Late Paleocene to middle Eocene calcareous nannofossil biochronology from the Shatsky Rise, Walvis Ridge and Italy. *Palaeogeography Palaeoclimatology Palaeoecology,* 57: 43-59.

Berberian M. & King G. (1981) - Towards a paleogeography and tectonic evolution of Iran. C*anadian journal of earth sciences,* 18(2): 210-265.

Bergen J., de Kaenel E., Blair S., Boesiger T. & Browning E. (2017) - Oligocene-Pliocene taxonomy and stratigraphy of the genus *Sphenolithus* in the circum North Atlantic Basin: Gulf of Mexico and ODP Leg 154. *Journal of Nannoplankton Research,* 37(2-3): 77-112.

Berggren W.A., Kent D.V., Swisher C.C. & Aubry M.-P. (1995) - A revised Cenozoic geochronology and chronostratigraphy. In: Berggren W.A. et al. (Eds.) - Geochronology, Time Scales and Global Stratigraphic Correlation. *Society for Sedimentary Geology Special Publication*, 54: 129-212.

Beydoun Z. (1988) - The Middle East: regional geology and petroleum resources. *Scientific Press, UK*, 155: 292 p.

Beydoun Z. (1991) - Arabian plate hydrocarbon geology and potential - a plate tectonic approach, American Association of Petroleum Geologists, Studies in Geology.

Beydoun Z. (1993) - Evolution of the northeastern Arabian plate margin and shelf: Hydrocarbon habitat and conceptual future potential. *Revue de l'Institut français du pétrole* 48(4): 311-345.

Bordenave M. & Hegre J. (2010) - Current distribution of oil and gas fields in the Zagros Fold Belt of Iran and contiguous offshore as the result of the petroleum systems. In: Leturmy P. & Robin C. (Eds.) - Tectonic and Stratigraphic Evolution of Zagros and Makran during the Mesozoic–Cenozoic. *Geological Society of London, London* (2010): 291-353.

Boukhary M., Abdelghany O., Bahr S. & Hussein-Kamel Y. (2005) - Upper Eocene larger foraminifera from the Dammam Formation in the border region of United Arab Emirates and Oman. *Micropaleontology,* 51(6): 487-504.

Bown P. & Young J. (1998) - Calcareous nannofossil biostratigraphy. *British Micropalaeontology Society Publication Service* 328 pp. (Chapman and Hall, 1998).

Bown P. R. & Dunkley Jones T. (2012) - Calcareous nannofossils from the Paleogene equatorial Pacific (IODP Expedition 320 Sites U1331-1334). *Journal of Nannoplankton Research,* 32(2): 3-51.

Bukry D. (1973) - Low-latitude coccolith biostratigraphic zonation. In: Edgar N.T., Saunders J.B. et al. - Initial Reports DSDP 15, Washington (U. S. Govt. Printing Office): 685-703.

Bukry D. (1975) - Coccolith and silicoflagellate stratigraphy, north western Pacific Ocean, *Deep Sea Drilling Project Leg. 32. Initial Rep. DSDP,* 32: 677-701.

Cherif O.H., Al-Rifaiy I.A. & El-Deeb W.Z. (1992) - Post-Nappes Early Tertiary Foraminiferal Paleoecology of the Northern Hafit Area, South of Al-Ain City (United Arab Emirates). *Micropaleontology*: 37-56.

Christian L. (1997) - Cretaceous subsurface geology of the Middle East region. *GeoArabia,* 2(3): 239-256.

Cotton L.J., Zakrevskaya E.Y., Van Der Boon A., Asatryan G., Hayrapetyan F., Israyelyan A., Krijgsman W., Less G., Monechi S. & Papazzoni C.A. (2017) - Integrated stratigraphy of the Priabonian (upper Eocene) Urtsadzor section, Armenia. *Newsletters on Stratigraphy,* 50(3): 269-295.

Dercourt J., Ricou L.E. & Vrielynck B. (1993) - Atlas Tethys, Paleoenvironmental Maps. Gauthier Villars, Paris: 307 pp.

Dunkley Jones T., Bown P.R., Pearson P.N., Wade B.S., Coxall H.K. & Lear C.H. (2008) - Major shifts in calcareous phytoplankton assemblages through the Eocene-Oligocene transition of Tanzania and their implications for low-latitude primary production." *Paleoceanography,* 23(4).

El-Khayal A. (1974) - Planktonic foraminiferal biostratigraphy of the Lower Tertiary Hibr Strata of northwest Saudi Arabia. *Bulletin of the Faculty of Science, Riyadh University,* 6: 174-194.

Farouk S., Ahmad F. & Smadi A.A. (2013) - Stratigraphy of the Middle Eocene-Lower Oligocene successions in northwestern and eastern Jordan. *Journal of Asian Earth Sciences,* 73: 396-408.

Farouk S., Faris M., Ahmad F. & Powell J.H. (2015) - New microplanktonic biostratigraphy and depositional sequences across the Middle-Late Eocene and Oligocene boundaries in eastern Jordan. *GeoArabia,* 20(3): 145-172.

Fioroni C., Villa G., Persico D. & Jovane L. (2015) - Middle Eocene-Lower Oligocene calcareous nannofossil biostratigraphy and paleoceanographic implications from Site 711 (equatorial Indian Ocean). *Marine Micropaleontology*, 118: 50-62.

Fornaciari E., Agnini C., Catanzariti R., Rio D., Bolla E.M. & Valvasoni E. (2010) - Mid-latitude calcareous nannofossil biostratigraphy, biochronology and evolution across the middle to late Eocene transition. *Stratigraphy* 7: 229-264.

Fornaciari E., Giusberti L., Luciani V., Tateo F., Agnini C., Backman J., Oddone M. & Rio D. (2007) - An expanded Cretaceous-Tertiary transition in a pelagic setting of the Southern Alps (central-western Tethys). *Palaeogeography Palaeoclimatology Palaeoecology,* 255: 98-131.

Galmed M.A., Nasr M.M. & Khater A.E.-S.M. (2020) - Petrology of Early Paleogene phosphorite deposits in Hazm Al-Jalamid, Northwest Saudi Arabia. *Arabian Journal of Geosciences,* 13(17): 829.

Ghandour I.M., Bălc R., Faris M., Helal S., Mosa G.A. & Aljahdali M.H. (2023) - New insight into the middle eocene calcareous nannoplankton biostratigraphy and

paleoenvironment from fayoum and beni suef areas, Egypt. *Rivista Italiana di Paleontologia e Stratigrafia,* 129(2).

Gradstein F., Ogg J.G., Schmitz M.D. & Ogg G.M. (2012) - The geologic time scale 2012, Elsevier.

Gradstein F.M. & Ogg J.G. (2020) - The chronostratigraphic scale. In Geologic time scale 2020: 21-32, Elsevier.

Guiraud R., Bosworth W., Thierry J. & Delplanque A. (2005) - Phanerozoic geological evolution of Northern and Central Africa: an overview. *Journal of African Earth Sciences,* 43(1-3): 83-143.

Haq B.U. & Al-Qahtani A.M. (2005) - Phanerozoic cycles of sea-level change on the Arabian Platform. *GeoArabia,* 10(2): 127-160.

Harzhauser M., Piller W.E. & Steininger F.F. (2002) - Circum-Mediterranean Oligo-Miocene biogeographic evolution - the gastropods' point of view. *Palaeogeography, Palaeoclimatology, Palaeoecology,* 183(1-2): 103-133.

Kamali M.R., Fathi M. & Mohsenian E. (2006) - Petroleum geochemistry and thermal modeling of Pabdeh Formation in Dezful Embayment.

Korin A., Allam S., Humphrey J.D., Amao A.O., Ayranci K., Najjar M.I., Bahameem A.A., Zalmout I.S., Memesh A.M. & Kaminski M.A. (2025) - The genus *Hantkenina* in Saudi Arabia: implications for biostratigraphy and paleoecology across the Bartonian–Priabonian transition. *Revue de Micropaléontologie*: 100844.

Lawa A. & Ghafur F.A. (2015) - Sequence stratigraphy and biostratigraphy of the prolific late Eocene, Oligocene and early Miocene carbonates from Zagros fold-thrust belt in Kurdistan region. *Arabian Journal of Geosciences,* 8(10): 8143-8174.

Lawver L.A. & Gahagan L.M. (2003) - Evolution of Cenozoic seaways in the circum-Antarctic region. *Palaeogeography, Palaeoclimatology, Palaeoecology,* 198(1-2): 11-37.

Martín-Martín M., Guerrera F., Tosquella J. & Tramontana M. (2021) - Middle Eocene carbonate platforms of the westernmost Tethys. *Sedimentary Geology,* 415: 105861.

Martini E. (1970) - Standard Palaeogene calcareous nannoplankton zonation. *Nature,* 226(5245): 560-561.

Martini E. (1971) - Standard Tertiary and Quaternary calcareous nannoplankton zonation. Proceedings second planktonic conference, Rome.

Meissner Jr. C., Dini S., Farasani A., Riddler G., Smith G., Griffin M. & Van Eck M. (1989) - Preliminary Geologic Map of the Thaniyat Turayf Quadrangle, Sheet 29C, Kingdom of Saudi Arabia. Open File Report USGS-OF-08-5, Ministry of Petroleum and Mineral Resources, US Geological Survey**:** 35 pp.

Meissner Jr. C., Riddler G., Van Eck M., Aspinall N., Farasani A. & Dini S. (1987) - Preliminary geologic map of the Turayf Quadrangle, sheet 31C, and part of the An Nabk quadrangle, sheet 31B, Kingdom of Saudi Arabia, US Geological Survey, Technical Report, Saudi Arabian Deputy Ministry for Mineral Resources: 89-336.

Messaoud J.H., Thibault N., Aljahdali M.H. & Yaich C. (2023) - Middle Eocene to early Oligocene biostratigraphy in the SW Neo-Tethys (Tunisia): large-scale correlations using calcareous nannofossil events and paleoceanographic implications. *Journal of African Earth Sciences,* 198: 104805.

Messaoud J.H., Thibault N., Yaich C., Monkenbusch J., Omar H., Jemai H.F.B. & Watkins D.K. (2020) - The Eocene-Oligocene Transition in the South-Western Neo-Tethys (Tunisia): Astronomical Calibration and Paleoenvironmental Changes. *Paleoceanography Paleoclimatology,* 35(8): e2020PA003887.

Miller K.G., Kominz M.A., Browning J.V., Wright J.D., Mountain G.S., Katz M.E., Sugarman P.J., Cramer B.S., Christie-Blick N. & Pekar S.F. (2005) - The Phanerozoic record of global sea-level change. *Science,* 310(5752): 1293-1298.

Murphy M.A. & Salvador A. (1999) - International stratigraphic guide - an abridged version. *Episodes Journal of International Geoscience*, 22(4): 255-271.

Nikfard M. (2023) - Lower Eocene carbonate ramp clinoforms of the southern Tethys; Zagros Foreland Basin, SW Iran: Sequence stratigraphy architecture, basin physiography and carbonate factory controlling parameters. *Basin Research,* 35(6): 2049-2077.

Okada H. & Bukry D. (1980) - Supplementary modification and introduction of code numbers to the low-latitude coccolith biostratigraphic zonation (Bukry, 1973; 1975). *Marine micropaleontology,* 5: 321-325.

Pälike H., Norris R.D., Herrle J.O., Wilson P.A., Coxall H.K., Lear C.H., Shackleton N.J., Tripati A.K. & Wade B.S. (2006) - The heartbeat of the Oligocene climate system. *Science*, 314(5807): 1894-1898.

Perch-Nielsen K. (1985) - Cenozoic calcareous nannofossils. In: Bolli H.M., Saunders J.B. & Perch-Nielsen K. (Eds.) - Plankton Stratigraphy. Cambridge University Press, Cambridge: 427-455.

Persico D. & Villa G. (2004) - Eocene-Oligocene calcareous nannofossils from Maud Rise and Kerguelen Plateau (Antarctica): paleoecological and paleoceanographic implications. *Marine Micropaleontology,* 52(1-4): 153-179.

Powers R., Ramirez L.F., Redmond C. & Elberg E. Jr. (1966) - Geology of the Arabian Peninsula: sedimentary geology of Saudi Arabia. *US Geological Survey*, 154 pp.

Premoli Silva I. & Jenkins D.G. (1993) - Decision on the Eocene-Oligocene boundary stratotype." *Episodes,* 16(3): 379-382.

Sadooni F.N. & Alsharhan A. (2019) - Regional stratigraphy, facies distribution, and hydrocarbons potential of the Oligocene strata across the Arabian Plate and Western Iran. *Carbonates and Evaporites,* 34(4): 1757-1770.

Senemari S. (2021) - Late Paleocene-Late Eocene Calcareous nannofossil biostratigraphy in the Zagros Basin (Iran), Tethyan realm. *Journal of African Earth Sciences,* 173: 104042.

Senemari S. & Jalili F. (2021) - Eocene to Oligocene nannofossils stratigraphy and environmental conditions in Izeh Province, Zagros Basin, East Tethys. *Journal of Palaeogeography,* 10(1): 10.

Senemari S. & Mahanipour A. (2023) - Calcareous nannofossils of the late Eocene to early Oligocene from the Pabdeh and Asmari transition in Dezful Embayment (southwestern Iran): Evidence of a climate cooling event. *Geological Journal,* 58(1): 356-367.

Sharland P., Archer R., Casey D., Davies R., Hall S., Heward A., Horbury A. & Simmons M. (2001) - Arabian Plate Sequence Stratigraphy. *GeoArabia Special Publication*, 2: 371.

Strougo A., Faris M., Abul-Nasr R.A., Gingerich P.D. & Haggag M.A. (2013) - Planktonic foraminifera and calcareous nannofossil biostratigraphy through the middle to late Eocene transition at Wadi Hitan, Fayum Province, Egypt.

Villa G., Fioroni C., Pea L., Bohaty S.M. & Persico D. (2008) - Middle Eocene–late Oligocene climate variability: Cal-

careous nannofossil response at Kerguelen Plateau, Site 748. *Marine Micropaleontology,* 69: 173-192.

Wade B.S., Aljahdali M.H., Mufrreh Y.A., Memesh A.M., AlSoubhi S.A. & Zalmout I.S. (2021) - Upper Eocene planktonic foraminifera from northern Saudi Arabia: implications for stratigraphic ranges. *Journal of Micropalaeontology,* 40(2): 145-161.

Wei W. & Wise Jr. S.W. (1989) - Paleogene calcareous nannofossil magnetobiostratigraphy: results from South Atlantic DSDP 516. *Marine Micropalentology,* 14: 119-152.

Weijermars R. (1999) - Surface geology, lithostratigraphy and Tertiary growth of the Dammam Dome, Saudi Arabia: a new field guide. *GeoArabia,* 4(2): 199-226.

Whittle G., Alsharhan A. & El Deeb W. (1995) - Bio-lithofacies and diagenesis in the early-middle oligocene of Abu Dhabi, United Arab Emirates. *Carbonates and Evaporites,* 10(1): 54-64.

Whittle G., Alsharhan A. & El Deeb W. (1996) - Facies analysis and early diagenesis of the middle-late Eocene dammam formation, Abu Dhabi, United Arab Emirates. *Carbonates and Evaporites,* 11(1): 32-41.

Zalmout I., Haptari M., Najjar M., Fadani M., Bahameem A., AlSobhi S., Mufarreh Y., Nabhan A., Masary A., Memesh A. & Gingerich P. (2023) - Marine Vertebrate Fossils of the Priabonian (Upper Eocene) Rashrashiyah Formation, Al Jawf Province, Northern Saudi Arabia. Middle East Oil, Gas and Geosciences Show (MEOS GEO), 19-21 February 2023, Bahrain.

Zhang Y., Li Z., Qin M., Bao Z., Li Z., Yi L. & Li G. (2021) - Sedimentology and stratigraphy sequence of the north of Saudi Arabia: implications for the evolution of the Neo-Tethys in the Late Cretaceous. *Geological Journal,* 56(3): 1510-1530.